interaction of RIG-I with ZNF598 or RNF135 in HEK293FT cells by immunoprecipitation (data not shown). RNF135 was previously annotated by the genome project and was recently found to be a cause of a genetic disease, neurofibromatosis, although its protein function was unknown. We renamed the protein Riplet (RING finger protein leading to RIG-I activation) based on the following functional analyses. Riplet was most similar to TRIM25 (60.8% sequence homology), in particular between their RING finger domains PRY or SPRY (Fig. 1*B*). Phylogenetic analysis also supported the notion that Riplet was similar to TRIM25 (Fig. 1*C*). Thus, we hypothesized that, like TRIM25, Riplet is a ubiquitin ligase.

Expression of Riplet—RIG-I mRNA is induced by type I IFN or poly(I-C) stimulation in mammalian cells. Unlike RIG-I, however, Riplet mRNA was basally expressed in HeLa and primary-cultured MRC-5 cells irrespective of stimulation (Fig. 1*D* and data not shown). On the other hand, when we treated bone marrow-derived dendritic cells with poly(I-C), the basal level of Riplet mRNA was increased by the stimulation (Fig. 1*D*), suggesting that the regulatory mechanism of Riplet expression somewhat differs among cell types, and that Riplet is expressed before virus infection in some cell types. Next we performed Northern blotting of human tissue RNA. Riplet mRNA was detected as a single band of 2.4 kbp, which is slightly longer than the RNF135 cDNA sequence deposited in GenBank™ (accession number AB470605). Human *RIPLET* is expressed in human skeletal muscle, spleen, kidney, placenta, prostate, stomach, thyroid, and tongue and also weakly expressed in heart thymus, liver, and lung (Fig. 1*E*).

Riplet Enhances RIG-I-mediated IFN-β Induction—At first we characterized the role of Riplet in RIG-I-mediated IFN inducing signaling by reporter gene analyses. When RIG-I was expressed in HEK293 cells, reporter auto-activation was observed even in the absence of exogenous stimulation (Fig. 2*A*) as reported previously (25, 26). Stimulation with poly(I-C) further enhanced the promoter. Co-expression of Riplet with RIG-I potentiated activation of the IFN-β promoter, whereas expression of Riplet alone resulted in only marginal activation (Fig. 2*A*). Detection of endogenous IFN-β mRNA confirmed that Riplet enhanced RIG-I-mediated activation of IFN-β transcription (supplemental Fig. S1). The enhancing role of Riplet in IFN-β promoter activation was also supported by activation of IRF-3 and NF-κB by Riplet (Fig. 2, *B* and *C*). In contrast, expression of a Riplet partial fragment (Riplet-DN) (70–432 amino acids) that lacked the N-terminal RING finger domain reduced promoter activation (Fig. 2*E*). The Riplet-L249fs mutant protein, which was isolated from neurofibromatosis patients (27), did not increase the RIG-I-mediated promoter activation (Fig. 2*D*). These data indicate that Riplet augments RIG-I-mediated IFN-β promoter activation, and that both the RING finger domain and the C-terminal region encoding the SPRY and PRY motifs are important for its function. Riplet (residues 70–432) acted as a dominant-negative form (hereafter called Riplet-DN) (Fig. 2, *E* and *F, left panel*). This functional feature of Riplet-DN was confirmed in Fig. 2, *B* and *C*, and was later confirmed through RIG-I co-precipitation and ubiquitination analyses (see Fig. 5*C* and supplemental Fig. S4*C*). Expression of Riplet-DN did not reduce TLR3 or MDA5 signaling (Fig. 2*E*), suggesting that Riplet-DN is specific for RIG-I signaling. Interestingly, the Riplet-DN only partially suppressed the function of the C-terminal deleted RIG-I (dRD), which is a constitutively active form (Fig. 2*F, right panel*), and RIG-I CARD-like region (dRIG-I)-mediated signaling in high or low dose transfection of dRIG-I was barely inhibited by overexpression of Riplet-DN (Fig. 2*F, center panel*). These data suggest that Riplet requires the RIG-I C-terminal domain (RD) and partial helicase region to activate RIG-I signaling.

Endogenous Riplet Promotes the RIG-I Signaling—We performed Riplet knockdown by siRNA Riplet using Lipofectamine 2000 reagents, instead of FuGENE HD, to reveal the function of endogenous Riplet. Two siRNAs (Riplet siRNA and Riplet si-1) that target different sites of the Riplet mRNA and two control siRNAs were used for knockdown analyses. The two siRNA or control siRNA were co-transfected with HA-tagged Riplet expression vector into HEK293 cells, and after 48 h, cell lysate was prepared and analyzed by Western blotting with anti-HA antibody detecting Riplet. The two siRNAs targeting Riplet abolished exogenously expressed Ripelt-HA, but control siRNA did not (supplemental Fig. S3). Likewise, both Riplet siRNA and Riplet si-1 specifically down-regulate the level of endogenous Riplet mRNA (Fig. 3, *A* and *B*).

Using the siRNA, we examined whether Riplet knockdown reduces RIG-I signaling. As expected, RIG-I-mediated IFN-β promoter activation was reduced by Riplet siRNA or Riplet si-1 compared with control siRNA (Fig. 3, *A* and *B*), indicating that Riplet is required for full activation of the RIG-I signaling. Vesicular stomatitis virus (VSV) is a negative-stranded RNA virus that induces IFN-β production via RIG-I (3). Although the

FIGURE 2. **Riplet enhances IFN-β signaling mediated by RIG-I.** *A*, Riplet enhances the promoter activation by RIG-I. HEK293 cells were transfected with plasmids encoding empty vector, RIG-I (0.1 μg) and Riplet (0.025, 0.05, or 0.1 μg) together with p125-luc (IFN-β promoter) reporter plasmid in 24-well plates. 24 h after transfection, the cells were treated with mock or poly(I-C) (50 μg/ml) for 4 h as described under "Experimental Procedures," and then luciferase activities of cell lysates were measured. *Closed* or *open boxes* represent poly(I-C) or mock stimulation, respectively. *B*, to examine the activation of IRF-3, RIG-I (0.1 μg), Riplet (0.1 μg), and/or Riplet-DN (0.1 μg),expressing vectors were transfected into HEK293 cells with reporter plasmids, GAL4 fused IRF-3 (0.05 μg), and the p55 UASG-luc reporter gene (0.05 μg), in which luciferase reporter gene is fused downstream of GAL4 protein-binding site, and therefore activated IRF-3 promotes the transcription of luciferase reporter gene. The cells were stimulated with poly(I-C) as described above (34). The total amount of transfected DNA (0.5 μg/well) was kept constant by adding empty vector (pEF-BOS). *C*, HEK293 cells were transfected with RIG-I (0.1 μg), Riplet (0.1 μg), and/or Riplet-DN (0.1 μg) expressing vectors together with the NF-κB reporter plasmid (0.1 μg), and 24 h later, the luciferase activities of cell lysates were measured. *D*, Riplet-L248fs, which lacks the C-terminal region, did not enhance the activation at all. HEK293 cells were transfected with the plasmids expressing wild-type Riplet (0.1 μg) or Riplet-L248fs (0.1 μg) together with RIG-I expressing vector (0.1 μg) and p125-luc reporter (0.1 μg). 24 h after transfection, cell were stimulated with poly(I-C), and the luciferase activities of cell lysates were determined as described above. *E*, RIG-I (0.1 μg), MDA5 (0.1 μg), or TLR3 (0.1 μg) expressing vectors were transfected into HEK293 cells with the plasmid encoding the Riplet-DN fragment (0.1, 0.2, or 0.3 μg) in 24-well plates. After 24 h, the cells were stimulated with 50 μg of poly(I-C) for 4 h, and relative luciferase activities were determined. *F*, Riplet-DN (100 ng) was co-transfected with full-length RIG-I (0, 50, 100, or 200 ng), RIG-I CARD-like region (dRIG-I) (0, 50, 100, or 200 ng), or C-terminal deleted RIG-I (RIG-I dRD) (0, 50, 100, or 200 ng) into HEK293 cells in 24-well plate, and reporter gene assays were carried out.

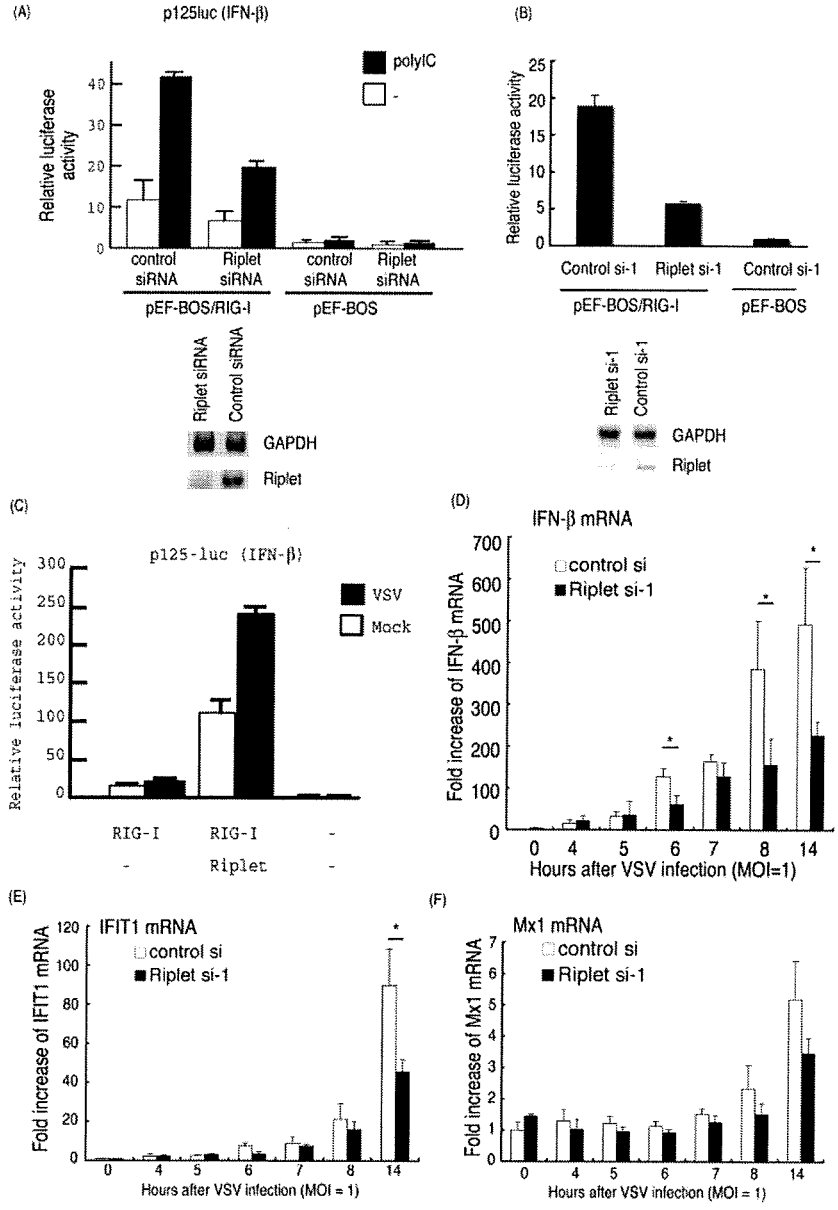

FIGURE 3. **Knockdown analyses of Riplet.** *A*, p125 luc reporter plasmid (0.1 μg), RIG-I expressing vector (0.1 μg), and Riplet siRNA or control siRNA (10 pmol), which were purchased from Funakoshi Co. Ltd., were transfected into HEK293 cells in a 24-well plate with Lipofectamine 2000, and 48 h after transfection, the cells were stimulated with poly(I-C) for 6 h, and the cell lysate was prepared, and luciferase activities were measured. RT-PCR was carried out using total RNA extracted from cells 48 h after transfection. *B*, p125 luc reporter plasmid (0.1 μg), RIG-I expressing vector (0.1 μg), and siRNA, Riplet si-1, or control si-1 (10 pmol), which were purchased from Applied Biosystems, were transfected into HEK293 cells with Lipofectamine 2000. 48 h after transfection, the cells were stimulated with poly(I-C) for 6 h. The cell lysate was prepared, and luciferase activities were measured. RT-PCR was carried out using total RNA extracted from cells 48 h after transfection. *C*, HEK293 cells were transfected with the plasmids expressing RIG-I (0.1 μg) and/or Riplet (0.1 μg) with p125 luc reporter plasmid (0.1 μg) in 24-well plates. After 24 h, the cells were infected with VSV (m.o.i. = 1) for 12 h. The luciferase activities of the cell lysates were measured. Expression of Riplet strongly enhanced IFN-β promoter activation by VSV through RIG-I. *D–F*, siRNA (control si- or Riplet si-1) were transfected into HEK293 cells, and after 48 h, the cells were infected with VSV at m.o.i. = 1. RNA was extracted at the indicated hours, and the quantitative PCR were carried out to detect the expression of IFN-β (*D*), IFIT-1 (*E*), or Mx1 (*F*) mRNA. *, $p < 0.05$. *GAPDH*, glyceraldehyde-3-phosphate dehydrogenase.

IFN-β promoter was only minimally activated by RIG-I in response to VSV (m.o.i. = 1) during the early phase of infection (<12 h), the activity was increased by RIG-I and Riplet (Fig. 3*C*). Riplet was silenced by siRNA and then VSV infected the cells. VSV-derived up-regulation of IFN-β mRNA was started around 6 h post-infection, and Riplet siRNA significantly suppressed the increase of IFN-β mRNA at 6 h (Fig. 3*D*). Because VSV infection is mainly sensed by RIG-I, this is consistent with the notion that Riplet promotes the RIG-I signaling. Other IFN-inducible genes, *IFIT1* and *MX1*, were expressed >8 h post-infection, and their expressions were also suppressed by Riplet siRNA (Fig. 3, *E* and *F*).

Riplet Exerts Protective Activity against Viral Infection—Next we examined the role of Riplet during viral infection. Riplet and/or RIG-I were transiently expressed in the human cells by FuGENE HD reagents, and then the cells were infected with VSV or poliovirus (a positive-stranded RNA virus). The viral titer of the supernatant was determined 24 h post-infection. Under our conditions, expression of RIG-I weakly inhibited VSV propagation. Co-expression of Riplet with RIG-I significantly suppressed VSV replication especially at low m.o.i., whereas Riplet alone did not suppress VSV (Fig. 4, *A* and *B*, *upper panel*). Therefore, a sufficient amount of RIG-I protein is required for Riplet to exert antivirus activity. This requirement of RIG-I is also observed in reporter gene analyses (Fig. 2). Under a similar setting, the antiviral effect of Riplet was marginally observed against poliovirus, which induces IFN-β largely via MDA5 (Fig. 4*B*, *lower panel*). To assess the importance of endogenous Riplet for antivirus effect of human cells, Riplet knockdown cells were infected with viruses. In Riplet knockdown cells, the VSV titer was consistently increased compared with the control ($p < 0.05$) (Fig. 4*C*, *left panel*). In addition, infection of Riplet knockdown cells with poliovirus resulted in only a slight increase in the poliovirus titer compared with the control ($p > 0.05$) (Fig. 4*C*, *right panel*). Because poliovirus is mainly recognized by MDA5 but not RIG-I, this marginal effect of Riplet on poliovirus infection was within expectation (3, 28).

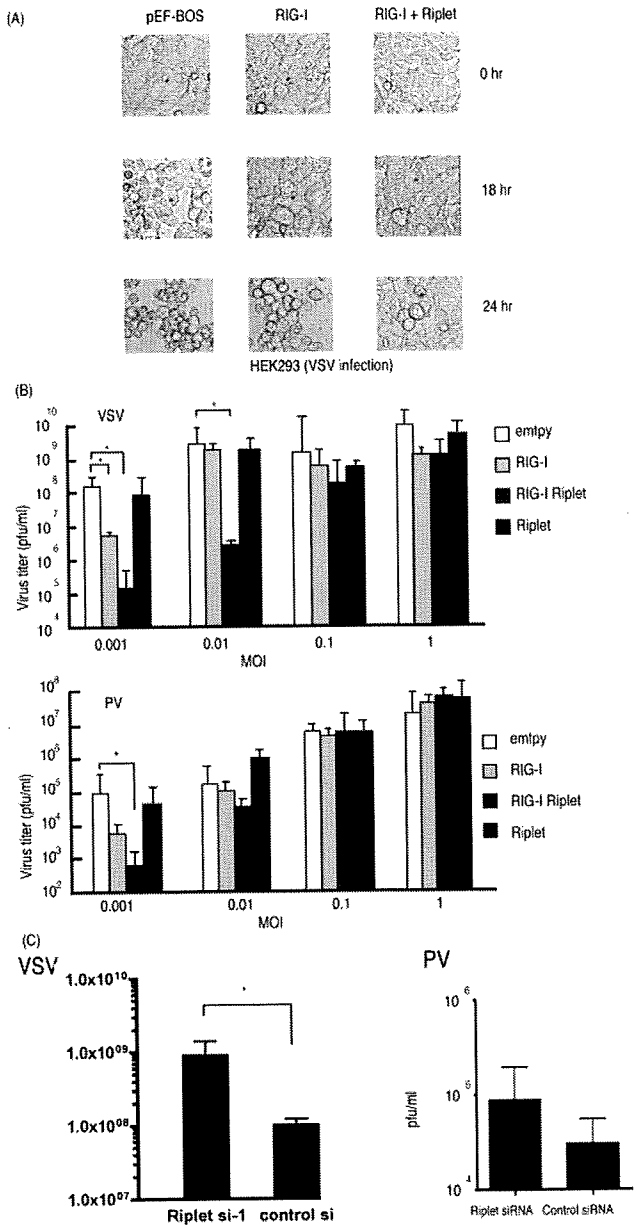

FIGURE 4. **Suppression of RNA viruses by Riplet.** *A*, HEK293 cells were transfected with RIG-I (0.1 μg) and/or Riplet (0.1 μg) expressing vectors. The total amount of transfected DNA (0.5 μg/well) in each well was kept constant by adding empty vector (pEF-BOS). 24 h after transfection, the cells were infected with VSV at m.o.i. = 0.1, and after 0, 18, or 24 h, CPE was observed by microscope. *B*, RIG-I (0.1 μg) and/or Riplet (0.1 μg) expressing plasmids were transfected to HEK293 cells in 24-well plates and incubated for 24 h. The total amount of transfected DNA (0.5 μg/well) in each well was kept constant by adding empty vector (pEF-BOS). The cells were infected with VSV (*upper panel*) or poliovirus (*PV*) (*lower panel*) at the indicated m.o.i. The viral titers in the culture media were measured 24 h after infection by plaque assay. *Error bars* represent standard deviation ($n = 3$). *, $p < 0.05$. *C*, control or Riplet knockdown HEK293 cells were infected with VSV (*left panel*) or poliovirus (*right panel*) at m.o.i. = 0.1. The viral titers in the culture media were measured 26 h after infection by plaque assays. Knockdown of Riplet induced higher VSV titers compared with control ($p < 0.05$), but the increase observed in poliovirus-infected Riplet knockdown cells was not significant ($p > 0.05$).

Riplet and Riplet-DN Bind the Helicase and RD Regions of RIG-I—Yeast two-hybrid analysis showed that a C-terminal region of Riplet bound to the C-terminal region of RIG-I. This cytoplasmic interaction between Riplet and RIG-I was confirmed by confocal microscopy in HeLa cells (supplemental Fig. S2). To further confirm the physical binding of Riplet to RIG-I in human cells, we carried out immunoprecipitation analyses. Full-length Riplet was co-immunoprecipitated with RIG-I (Fig. 5*B*), indicating that Riplet binds directly to RIG-I in human cells.

To determine the region responsible for the RIG-I-Riplet interaction, we constructed a RIG-I and Riplet deletion series as shown in Fig. 5*A*. Riplet-DN also bound to RIG-I (Fig. 5, *B* and *C*), indicating that the RING finger domain is dispensable for the RIG-I-Riplet interaction. This is consistent with the notion that the RING finger domain in ubiquitin ligase proteins is required for their interactions with ubiquitin-conjugating enzymes (29). Unlike TRIM25, Riplet and Riplet-DN failed to co-precipitate the two CARD domains of RIG-I (dRIG-I) (Fig. 5*D*). However, co-precipitation of the RIG-IC or RIG-RD fragments was observed (Fig. 5, *E* and *F*). RD-deleted RIG-I (RIG-I dRD) weakly associated with Riplet (Fig. 5*G*). Taken together, Riplet preferentially binds the RD and also weakly associates with the helicase region of RIG-I with its C terminus. Reporter gene analyses show that Riplet-DN only weakly suppresses RIG-I signaling and barely suppresses dRIG-I, which contains neither helicase nor RD region. Therefore, the physical interaction is correlated with the results of reporter activity.

Riplet Promotes Ubiquitination of RIG-I—Because Riplet shares 60% sequence similarity with TRIM25, we hypothesized that Riplet ubiquitinates RIG-I and that this modification leads to activation of RIG-I signaling. To test this hypothesis, we examined RIG-I ubiquitination. As expected, ubiquitination of RIG-I was increased by co-expression of Riplet under two different conditions (Fig. 6, *A* and *B*). The quantity of RIG-I ubiquitination was significantly high in the presence of Riplet (Fig. 6*C*). RIG-I ubiquitination was suppressed if Riplet was replaced with Riplet-DN (Fig. 6*D* and supplemental Fig. S4*C*). However, unlike TRIM25, Riplet binds to the C-terminal region of RIG-I. Therefore, we examined whether Riplet ubiquitinates the C-terminal region. We found that ubiquitination of RIG-IC was enhanced by Riplet expression (Fig. 6*E*). Both RIG-I dRD and RIG-I RD were also ubiquitinated by expression of Riplet (Fig. 6*F*; supplemental Fig. S4*A* and S5), suggesting that Riplet promotes ubiquitination of the helicase and RD domains of RIG-I in a manner distinct from TRIM25.

Ubiquitin is polymerized through its lysine residue. Lys-63-linked polyubiquitination is frequently observed in signal transduction pathways (30). In contrast, Lys-48-linked polyubiquitination usually leads to the degradation of protein through the proteasome. Indeed, TRIM25-mediated Lys-63-linked polyubiquitination activates the CARD-like region of RIG-I, and RNF125-mediated Lys-48-linked polyubiquitination leads to the degradation of RIG-I (23, 25). We used K48R or K63R mutated ubiquitin and found that K48R was incorporated normally into RIG-IC, whereas polyubiquitination was decreased by K63R (supplemental Fig. S4*B*). K63R mutation abolished RIG-I RD polyubiquitination by Riplet (Fig. 6*F*). These data

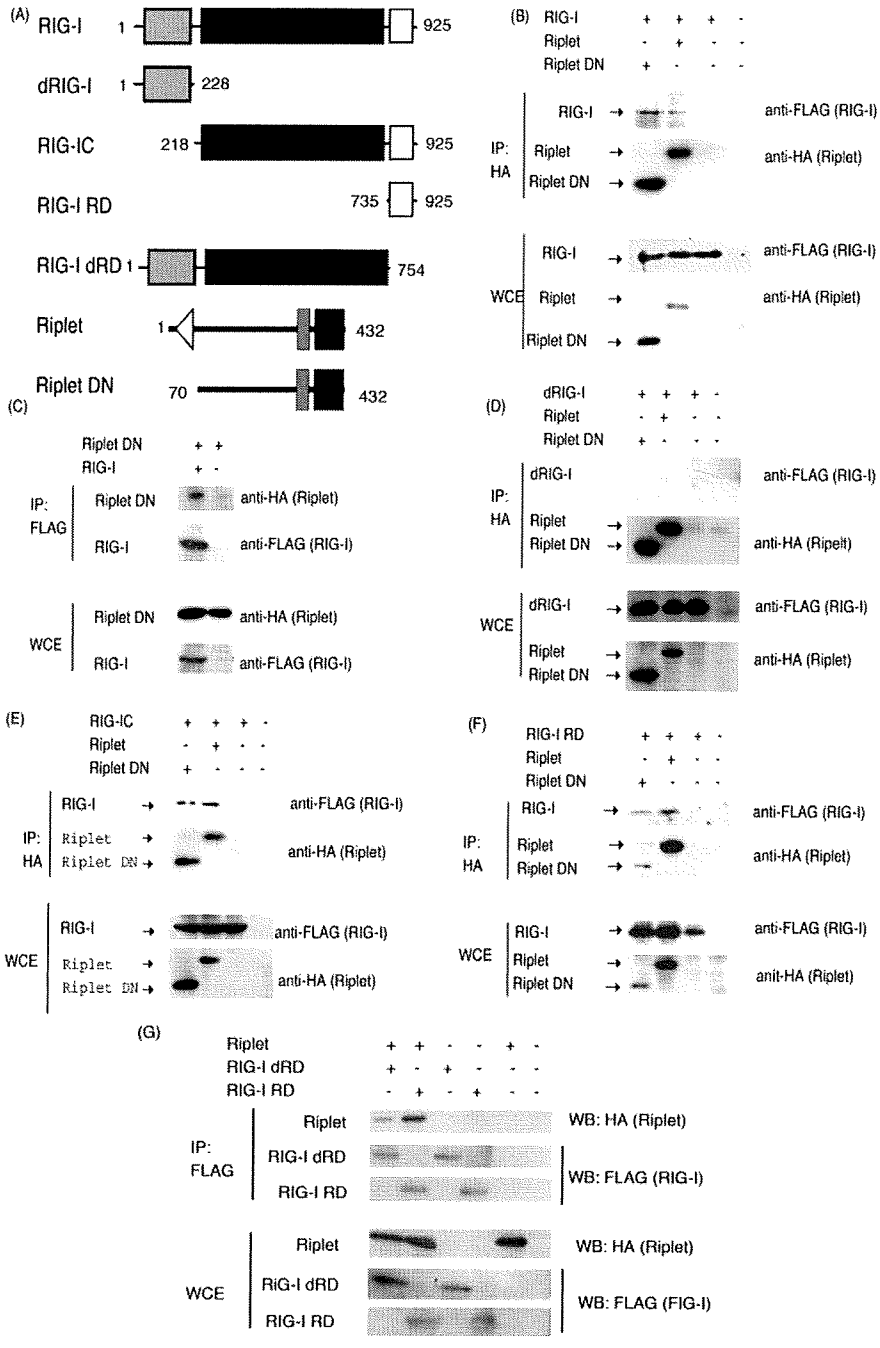

FIGURE 5. **Physical interaction of Riplet with RIG-I.** *A*, schematic representation of RIG-I or Riplet fragments used for immunoprecipitation analyses. *B*, HA-tagged Riplet (0.4 μg) or Riplet-DN (0.4 μg) were transfected into HEK293FT cells in a 6-well plate with FLAG-tagged RIG-I (0.4 μg). HA-tagged Riplet or Riplet-DN were immunoprecipitated (*IP*) with anti-HA antibodies, and samples were analyzed by Western blotting (*WB*) using an anti-FLAG or anti-HA antibody. The total amount of transfected DNA (2 μg/well) was kept constant by adding empty vector (pEF-BOS). *C*, HA-tagged Riplet-DN (0.4 μg) and FLAG-tagged RIG-I (0.4 μg) were transfected into HEK293FT cells in a 6-well plate. RIG-I was immunoprecipitated with anti-FLAG antibody, and samples were analyzed by Western blotting using an anti-FLAG or -HA antibody. The total amount of transfected DNA (2 μg/well) was kept constant by adding empty vector (pEF-BOS). *D–F*, interaction of HA-tagged Riplet or Riplet-DN with FLAG-tagged dRIG-I (*D*), RIG-IC (*E*), or RIG-I RD (*F*) was examined using immunoprecipitation assays. The proteins were expressed in HEK293FT cells, and HA-tagged Riplet was immunoprecipitated with anti-HA antibody, and samples were analyzed by Western blotting using an anti-FLAG or -HA antibody. *G*, FLAG-tagged RIG-I RD (0.4 μg) or RIG-I dRD (0.4 μg) was transfected with HA-tagged Riplet (0.4 μg) into HEK293 FT cells in a 6-well plate, and 24 h after transfection, immunoprecipitation was performed with anti-FLAG antibody and analyzed by Western blotting. The total amount of transfected DNA (2 μg/well) was kept constant by adding empty vector (pEF-BOS). *WCE*, whole cell extract.

indicates that Riplet mediates Lys-63-linked polyubiquitination of the RIG-I C-terminal helicase and RD region. Because Riplet-DN reduced the RIG-I-mediated signaling, we examined whether Riplet-DN reduced the RIG-I ubiquitination. As expected, Riplet-DN reduced RIG-I ubiquitination (Fig. 6*D* and supplemental Fig. S4*C*). These ubiquitination assay data are consistent with the notion that Riplet-mediated Lys-63-linked polyubiquitination of RIG-I is required for full activation of RIG-I signaling.

We tried to determine the ubiquitination sites of RIG-I using Lys-to-Ala (KA)-converting mutants. RIG-I has 25 Lys residues in its C-terminal region. These Lys residues of RIG-I were in turn mutated to Ala, and the degree of ubiquitination and IFN-β-inducing activity were determined with each mutant. RIG-I-mediated IFN-β promoter activation was normally augmented by co-expression of Riplet and 3KA RIG-I. Co-expression of Riplet and 5KA, however, and the ubiquitination level of RIG-I and IFN-β-inducing activity were simultaneously decreased (Fig. 7, *A* and *C*). Riplet-dependent augmentation of IFN-β promoter activation was largely suppressed when RIG-I was replaced with 5KA RIG-I (Fig. 7*B*). Therefore, Lys-849 and Lys-851 of RIG-I were crucial for RIG-I ubiquitination by Riplet. The results confirmed the importance of ubiquitination of specific Lys residues in the C-terminal region of RIG-I and for RIG-I-mediated IFN-β induction.

DISCUSSION

RIG-I plays a central role in the recognition of cytoplasmic viral RNA and is regulated by modification by small modifier ubiquitin or ubiquitin-like protein, ISG15. TRIM25 mediates Lys-63-linked polyubiquitination, which is essential for RIG-I activation (23), and RNF125 mediates Lys-48-linked polyubiquitination (25). RIG-I also harbors ISG15 modification, although the role of ISG15 modification *in vivo* remains to be deter-

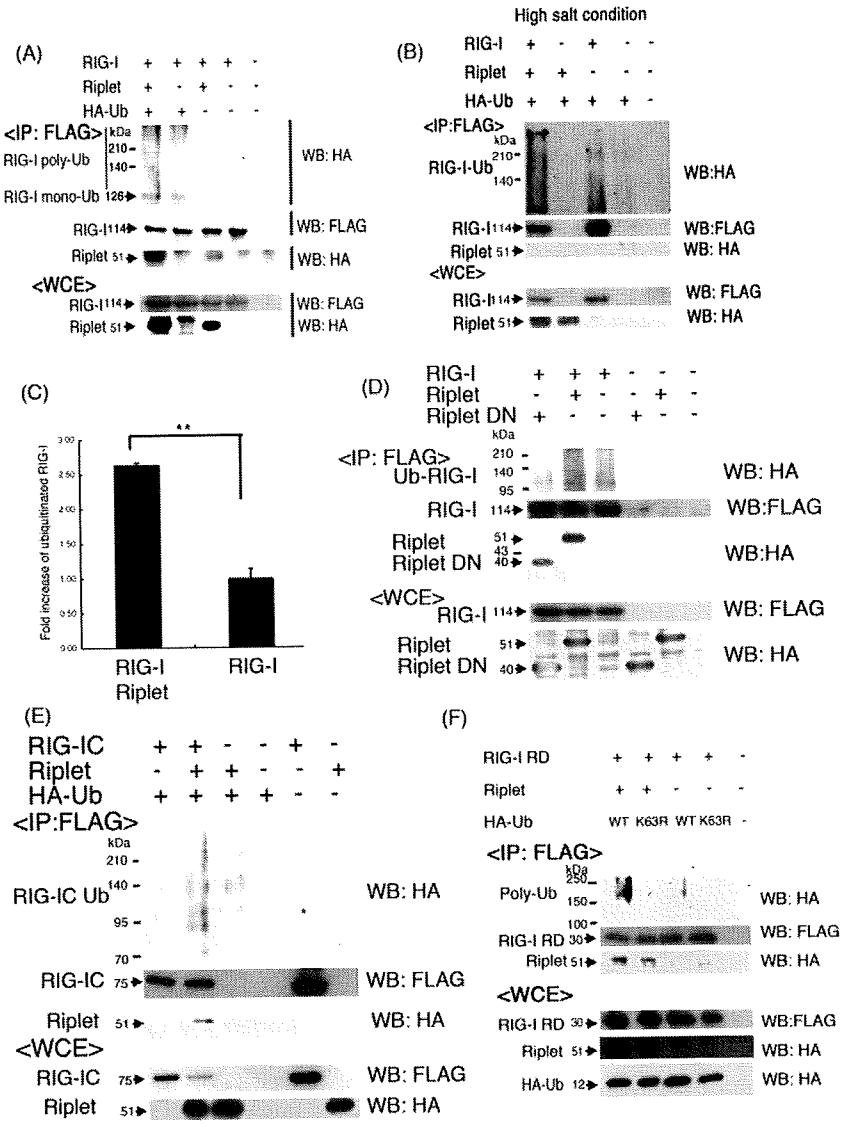

FIGURE 6. **Ubiquitination of RIG-I by Riplet.** *A* and *B*, FLAG-tagged RIG-I (0.4 μg), Riplet (0.4 μg), and HA-tagged ubiquitin (0.4 μg) expressing vectors were transfected into HEK293FT cells in 6-well plates. The total amount of transfected DNA (2 μg/well) was kept constant by adding empty vector (pEF-BOS). FLAG-tagged RIG-I was immunoprecipitated (*IP*) using an anti-FLAG antibody, and washed with the buffer containing 150 mM NaCl (*A*) or 1 M NaCl (*B*). The immunoprecipitates were separated with 8% acrylamide gel and analyzed by Western blotting (*WB*) using antibodies against HA tag (ubiquitin) or FLAG (RIG-I). Riplet was co-immunoprecipitated with FLAG-tagged RIG-I in *A* but could not co-immunoprecipitate in *B* because of high salt condition. Expression of Riplet enhanced the ubiquitination of RIG-I. Different gel conditions were employed in *A* and *B*. *C*, ubiquitinated RIG-I was quantitated with NIH image software. **, $p < 0.01$. *D*, FLAG-tagged RIG-I (0.4 μg) was transfected into HEK293 FT cells in a 6-well plate with HA-tagged Riplet (0.4 μg) or Riplet-DN (0.4 μg) and HA-tagged ubiquitin, and immunoprecipitation was carried out with anti-FLAG antibody. The total amount of transfected DNA (2 μg/well) was kept constant by adding empty vector (pEF-BOS). The samples were analyzed with 10% acrylamide gel to clearly separate Riplet from Riplet-DN and stained by Western blotting. *E*, ubiquitination of RIG-IC was also promoted by Riplet expression. HEK293FT cells were transfected with the plasmids encoding RIG-IC (0.4 μg), Riplet (0.4 μg), and/or HA-tagged ubiquitin (0.4 μg) in a 6-well plate, and 24 h after transfection, cell lysates were prepared. The total amount of transfected DNA (2 μg/well) was kept constant by adding empty vector (pEF-BOS). FLAG-tagged RIG-ICs were immunoprecipitated with anti-FLAG antibodies, and the proteins were analyzed by Western blotting. *F*, Ub-K63R are HA-tagged ubiquitin in which the lysine 3 residues were substituted with arginine. The HA-tagged Ub-K63 expressing vectors (1.2 μg), FLAG-tagged RIG-IC (0.4 μg), and/or Riplet (0.4 μg) were transfected into HEK293FT cells in 6-well plates and analyzed as shown in *A–D*. The total amount of transfected DNA (2 μg/well) was kept constant by adding empty vector (pEF-BOS). Ub-K63R was not incorporated into polyubiquitin chain of RIG-I RD. *WCE*, whole cell extract.

mined (21, 22, 31). Although Riplet and TRIM25 share 60% sequence similarity, the ubiquitination of RIG-I by Riplet is distinct from that by TRIM25; Riplet ubiquitinates the C-terminal region of RIG-I, whereas TRIM25 ubiquitinates its CARD-like region. These findings are also supported by the fact that neither Riplet nor Riplet-DN promoted or inhibited the activation of the IFN-β promoter by expression of the RIG-I CARD-like region (data not shown). It has been reported that ubiquitination of the CARD-like region of RIG-I by TRIM25 is critical for RIG-I-IPS-1 signaling (23). However, how this CARD ubiquitination is essential for activation of IPS-1 by RIG-I remains undetermined. Here we emphasize the importance of RIG-I C-terminal ubiquitination for IFN-β induction and the antiviral response. Because the C-terminal RD region inhibits the IFN inducing activity of the CARD-like region of RIG-I, it is reasonable that RIG-I C-terminal ubiquitination by Riplet inhibits the conversion from the active to inactive form of RIG-I protein after binding to viral RNA. This initial stabilization of RIG-I via ubiquitination by Riplet would provide a sufficient structure for RIG-I to maintain the accessibility to TRIM25 and facilitate TRIM25-mediated ubiquitination of the CARD-like region of RIG-I, which may lead to potential activation of IPS-1.

RIG-I is an IFN-inducible RNA helicase that is expressed at extremely low levels in resting cells (6). Initial penetration of viruses allows generation of 5′-triphosphate RNA and/or double strand RNA followed by induction of IFN-β production. This early response to viral infections triggers up-regulation of RIG-I/MDA5 and TLR3, leading to robust IFN-β production (3, 32, 33). We favor the interpretation of our present findings that during the early stages of viral infection with trace amounts of RIG-I and viral RNAs, Riplet helps host cells rearrange RIG-I conformation to activate IPS-1. This issue will need further proof because it is difficult to

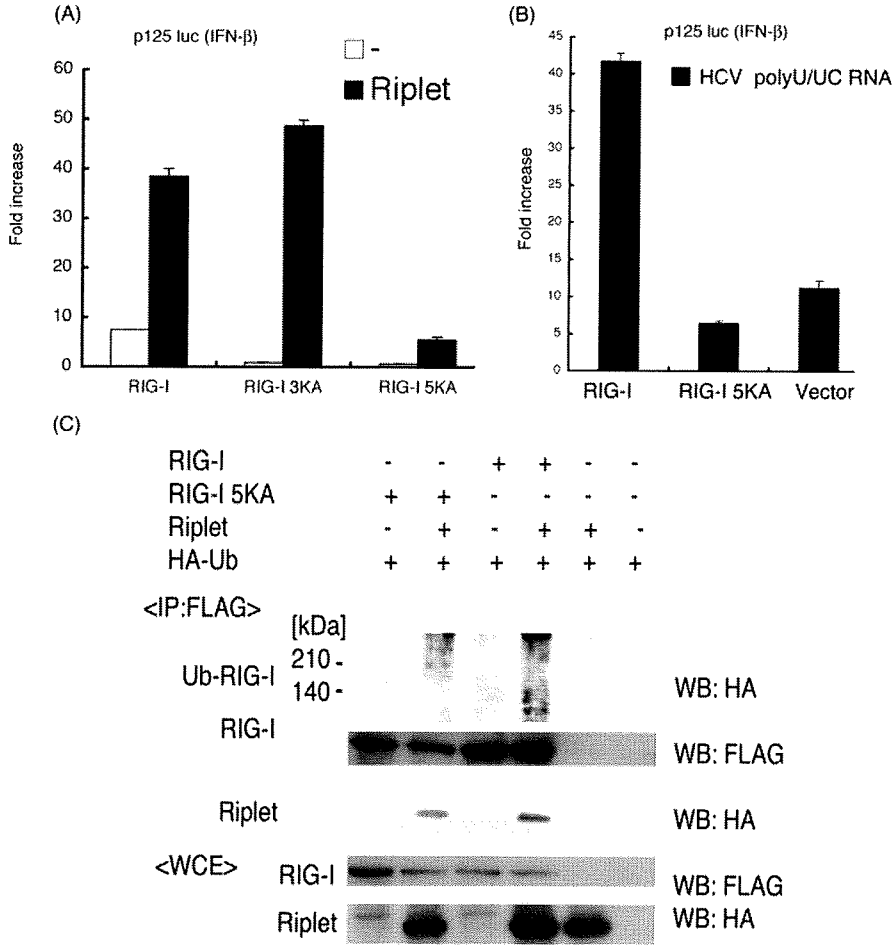

FIGURE 7. **The C-terminal two lysine residues of RIG-I are important for ubiquitination by Riplet.** *A*, RIG-I C-terminal lysine residues were substituted with alanine. RIG-I 3KA mutant protein harbors the triple mutations, K888A, K907A, and K909A. The five lysine residues, Lys-849, Lys-851, Lys-888, Lys-907, and Lys-909, were replaced with alanine in RIG-I 5KA mutant. The plasmid carrying wild-type (100 ng/well), RIG-I 3KA (100 ng/well), RIG-I 5KA (100 ng), or Riplet (100 ng) were transfected into HEK293 cells in a 24-well plate together with p125 luc reporter plasmid (100 ng/well). The amount of transfected DNA was kept constant by adding empty vector. After 24 h, the luciferase activities were measured. *B*, wild-type RIG-I (100 ng), RIG-I 5KA mutant (100 ng), or empty vector (100 ng) was transfected into HEK293 cells in a 24-well plate together with p125 luc reporter plasmids and HCV 3′-untranslated region poly(U/UC) RNA (25 ng), which is synthesized in *in vitro* transcription by T7 RNA polymerase. The amount of transfected DNA was kept constant by adding empty vector. 24 h after transfection, luciferase activities were measured. RIG-I 5KA mutant hardly responded to poly(U/UC) RNA. *C*, to observe the ubiquitinated RIG-I more clearly, we used 800 ng/well of Riplet and HA-Ub expression vector for the following transfection. HEK293FT cells in a 6-well plate were transfected with the plasmids encoding RIG-I (400 ng/well), RIG-I 5KA (400 ng/well), Riplet (800 ng/well), and/or HA-Ub (800 ng/well). The total amount of DNA was kept constant by adding the empty vector. 24 h after the transfection, the cell lysates were prepared, and the immunoprecipitation was carried out using anti-FLAG antibodies. The immunoprecipitates were analyzed by Western blotting with anti-HA or FLAG antibodies.

visualize RNRs and viral RNAs in the early infection stage and to understand the mechanisms that allow viruses to uncoat into naked viral RNA and to replicate.

We have provided several lines of evidence indicating that Riplet complements RIG-I-mediated IFN-β induction upon viral infection by both Riplet siRNA and overexpression analyses. The C-terminal lysines (849 and 851) of RIG-I are critical for Riplet-mediated RIG-I ubiquitination. However, our data indicate that Riplet alone was unable to induce IFN-β production and essentially required RIG-I to confer IFN-β induction. Furthermore, Riplet is not ubiquitously distributed over the organs tested. Ubiquitination of RIG-I induced by poly(I-C) or viruses was accelerated in cells pre-transfected with Riplet. Hence, Riplet works case-sensitive to up-regulate RIG-I antiviral activity predominantly in some organs. The physiological meaning of this response will be clarified by knock-out study.

Unexpectedly, the siRNA experiments were not robust with regard to VSV replication. Possible explanations for this are as follows: 1) the degree of gene silencing is not so profound that the proteins remain in the cells; 2) there are a number of virus-mediated IFN-inducing pathways capable of compensating each other, so that disruption of one factor does not cause a profound effect on VSV replication. Furthermore, in VSV-infected Riplet-knockdown cells, IFN-β levels were reduced even at m.o.i. = 1 (Fig. 3*D*), and accordingly, virus susceptibility was increased at m.o.i. = 0.1 (Fig. 4*C*), whereas in Riplet-overexpressing cells, antiviral activity was observed only at low m.o.i. (Fig. 4*B*). We used different transfection reagents and cell conditions in the knockdown and overexpression experiments to obtain high transfection efficiency in each. These conditional differences in knockdown and overexpression analyses might cause part of the discrepancy between the two results on Riplet antiviral activity. Another possibility to explain the apparent inconsistencies between overexpression and knockdown analyses is that high amounts of Riplet efficiently activate the RIG-I signaling, but low amounts are insufficient for RIG-I activation in high m.o.i.-infecting human cells. High amounts of Riplet with overexpressed RIG-I would confer the ability on cells to respond to very low amounts of VSV as observed in the low m.o.i. experiments. Again, *riplet* knock-out mice would reveal whether it is absolutely required for potential RIG-I activation.

How viral RNAs select RIG-I rather than dicers or the translation machinery is also unknown. During natural infection it is likely that the number of the initial invading virions would be at most several copies/cell. Uncoated viral RNA may assemble a complex consisting of viral and host molecules required for replication. We assume that cells are equipped with various

molecular arms to sensitively detect viral RNA. The molecular complexes sensing viral RNA may not be so simple that we will be able to identify more molecules than Riplet as enhancers for integral RNA recognition. In either case, yeast screening will be a good strategy to pick up such proteins in other RNA recognition systems. A molecular switch selecting IFN induction by virus RNA will then be clarified.

We show that the ubiquitination sites targeted by Riplet are the helicase and RD domains of RIG-I but not its CARD-like domains in contrast to TRIM25. Riplet may be a complement factor of the reported TRIM25 function for RIG-I activation (23). A previous report (25) failed to polyubiquitinate the RIG-I protein by TRIM25 alone. If Riplet were added to TRIM25 for RIG-I ubiquitination in the previous study, Riplet would have enabled TRIM25 to polyubiquitinate the RIG-I CARD-like region. Further studies using TRIM25 and Riplet will be required to clarify this point.

Based on our results, we propose that RIG-I-like receptors form a molecular complex that efficiently recognizes low copy numbers of viral RNA. Riplet is implicated in the RIG-I complex to enhance viral RNA response in some organs. In this context, MDA5-associated molecules might also exist in the cytoplasm to augment IFN output. Although MDA5 possesses the RD domain, it fails to recruit Riplet (data not shown) or augment IFN-β-induction in conjunction with Riplet (Fig. 2*E*). Because RLR-associated molecules naturally reside in cells and facilitate inhibition of low dose viral infection until RLRs become expressed, they may be useful therapeutic targets for an early phase antiviral immunotherapy.

Acknowledgments—We thank Dr. M. Sasai in our laboratory for technical instructions for assay of RIG-I functions and Drs. K. Shimotohno (Keio University), T. Taniguchi (University of Tokyo), and T. Fujita (Kyoto University) for their critical discussions.

REFERENCES

1. Takeuchi, O., and Akira, S. (2008) *Curr. Opin. Immunol.* **20,** 17–22
2. Honda, K., Takaoka, A., and Taniguchi, T. (2006) *Immunity* **25,** 349–360
3. Kato, H., Takeuchi, O., Sato, S., Yoneyama, M., Yamamoto, M., Matsui, K., Uematsu, S., Jung, A., Kawai, T., Ishii, K. J., Yamaguchi, O., Otsu, K., Tsujimura, T., Koh, C. S., Reis e Sousa, C., Matsuura, Y., Fujita, T., and Akira, S. (2006) *Nature* **441,** 101–105
4. Venkataraman, T., Valdes, M., Elsby, R., Kakuta, S., Caceres, G., Saijo, S., Iwakura, Y., and Barber, G. N. (2007) *J. Immunol.* **178,** 6444–6455
5. Yoneyama, M., Kikuchi, M., Matsumoto, K., Imaizumi, T., Miyagishi, M., Taira, K., Foy, E., Loo, Y. M., Gale, M., Jr., Akira, S., Yonehara, S., Kato, A., and Fujita, T. (2005) *J. Immunol.* **175,** 2851–2858
6. Yoneyama, M., Kikuchi, M., Natsukawa, T., Shinobu, N., Imaizumi, T., Miyagishi, M., Taira, K., Akira, S., and Fujita, T. (2004) *Nat. Immunol.* **5,** 730–737
7. Hornung, V., Ellegast, J., Kim, S., Brzozka, K., Jung, A., Kato, H., Poeck, H., Akira, S., Conzelmann, K. K., Schlee, M., Endres, S., and Hartmann, G. (2006) *Science* **314,** 994–997
8. Pichlmair, A., Schulz, O., Tan, C. P., Naslund, T. I., Liljestrom, P., Weber, F., and Reis e Sousa, C. (2006) *Science* **314,** 997–1001
9. Saito, T., Hirai, R., Loo, Y. M., Owen, D., Johnson, C. L., Sinha, S. C., Akira, S., Fujita, T., and Gale, M., Jr. (2007) *Proc. Natl. Acad. Sci. U. S. A.* **104,** 582–587
10. Kawai, T., Takahashi, K., Sato, S., Coban, C., Kumar, H., Kato, H., Ishii, K. J., Takeuchi, O., and Akira, S. (2005) *Nat. Immunol.* **6,** 981–988
11. Meylan, E., Curran, J., Hofmann, K., Moradpour, D., Binder, M., Bartenschlager, R., and Tschopp, J. (2005) *Nature* **437,** 1167–1172
12. Seth, R. B., Sun, L., Ea, C. K., and Chen, Z. J. (2005) *Cell* **122,** 669–682
13. Xu, L. G., Wang, Y. Y., Han, K. J., Li, L. Y., Zhai, Z., and Shu, H. B. (2005) *Mol. Cell* **19,** 727–740
14. Rothenfusser, S., Goutagny, N., DiPerna, G., Gong, M., Monks, B. G., Schoenemeyer, A., Yamamoto, M., Akira, S., and Fitzgerald, K. A. (2005) *J. Immunol.* **175,** 5260–5268
15. Loo, Y. M., Fornek, J., Crochet, N., Bajwa, G., Perwitasari, O., Martinez-Sobrido, L., Akira, S., Gill, M. A., Garcia-Sastre, A., Katze, M. G., and Gale, M., Jr. (2008) *J. Virol.* **82,** 335–345
16. Komuro, A., and Horvath, C. M. (2006) *J. Virol.* **80,** 12332–12342
17. McWhirter, S. M., Tenoever, B. R., and Maniatis, T. (2005) *Cell* **122,** 645–647
18. Saha, S. K., Pietras, E. M., He, J. Q., Kang, J. R., Liu, S. Y., Oganesyan, G., Shahangian, A., Zarnegar, B., Shiba, T. L., Wang, Y., and Cheng, G. (2006) *EMBO J.* **25,** 3257–3263
19. Kayagaki, N., Phung, Q., Chan, S., Chaudhari, R., Quan, C., O'Rourke, K. M., Eby, M., Pietras, E., Cheng, G., Bazan, J. F., Zhang, Z., Arnott, D., and Dixit, V. M. (2007) *Science* **318,** 1628–1632
20. Lin, R., Yang, L., Nakhaei, P., Sun, Q., Sharif-Askari, E., Julkunen, I., and Hiscott, J. (2006) *J. Biol. Chem.* **281,** 2095–2103
21. Zhao, C., Denison, C., Huibregtse, J. M., Gygi, S., and Krug, R. M. (2005) *Proc. Natl. Acad. Sci. U. S. A.* **102,** 10200–10205
22. Arimoto, K., Konishi, H., and Shimotohno, K. (2008) *Mol. Immunol.* **45,** 1078–1084
23. Gack, M. U., Shin, Y. C., Joo, C. H., Urano, T., Liang, C., Sun, L., Takeuchi, O., Akira, S., Chen, Z., Inoue, S., and Jung, J. U. (2007) *Nature* **446,** 916–920
24. Urano, T., Saito, T., Tsukui, T., Fujita, M., Hosoi, T., Muramatsu, M., Ouchi, Y., and Inoue, S. (2002) *Nature* **417,** 871–875
25. Arimoto, K., Takahashi, H., Hishiki, T., Konishi, H., Fujita, T., and Shimotohno, K. (2007) *Proc. Natl. Acad. Sci. U. S. A.* **104,** 7500–7505
26. Sasai, M., Shingai, M., Funami, K., Yoneyama, M., Fujita, T., Matsumoto, M., and Seya, T. (2006) *J. Immunol.* **177,** 8676–8683
27. Douglas, J., Cilliers, D., Coleman, K., Tatton-Brown, K., Barker, K., Bernhard, B., Burn, J., Huson, S., Josifova, D., Lacombe, D., Malik, M., Mansour, S., Reid, E., Cormier-Daire, V., Cole, T., and Rahman, N. (2007) *Nat. Genet.* **39,** 963–965
28. Barral, P. M., Morrison, J. M., Drahos, J., Gupta, P., Sarkar, D., Fisher, P. B., and Racaniello, V. R. (2007) *J. Virol.* **81,** 3677–3684
29. Seol, J. H., Feldman, R. M., Zachariae, W., Shevchenko, A., Correll, C. C., Lyapina, S., Chi, Y., Galova, M., Claypool, J., Sandmeyer, S., Nasmyth, K., Deshaies, R. J., Shevchenko, A., and Deshaies, R. J. (1999) *Genes Dev.* **13,** 1614–1626
30. Pickart, C. M. (2004) *Cell* **116,** 181–190
31. Kim, M. J., Hwang, S. Y., Imaizumi, T., and Yoo, J. Y. (2008) *J. Virol.* **82,** 1474–1483
32. Alexopoulou, L., Holt, A. C., Medzhitov, R., and Flavell, R. A. (2001) *Nature* **413,** 732–738
33. Tanabe, M., Kurita-Taniguchi, M., Takeuchi, K., Takeda, M., Ayata, M., Ogura, H., Matsumoto, M., and Seya, T. (2003) *Biochem. Biophys. Res. Commun.* **311,** 39–48
34. Yoneyama, M., Suhara, W., Fukuhara, Y., Fukuda, M., Nishida, E., and Fujita, T. (1998) *EMBO J.* **17,** 1087–1095

FEBS Letters 583 (2009) 1434–1438

FEBS Letters

journal homepage: www.FEBSLetters.org

Oncostatin M synergistically inhibits HCV RNA replication in combination with interferon-α

Masanori Ikeda *, Kyoko Mori, Yasuo Ariumi, Hiromichi Dansako, Nobuyuki Kato

Department of Tumor Virology, Okayama University Graduate School of Medicine, Dentistry and Pharmaceutical Sciences, 2-5-1 Shikata-cho, Okayama 700-8558, Japan

ARTICLE INFO

Article history:
Received 23 February 2009
Revised 17 March 2009
Accepted 24 March 2009
Available online 28 March 2009

Edited by Hans-Dieter Klenk

Keywords:
Oncostatin M
Interferon
Hepatitis C virus

ABSTRACT

Oncostatin M (OSM), a member of the interleukin-6 family, possesses various functions, including hepatocyte differentiation and suppression of melanoma cell growth. Here, we report anti-hepatitis C virus (HCV) activity of OSM as a new function of this cytokine. OSM possessed marked anti-HCV activity (50% effective concentration: 0.71 ng/ml) in an HCV RNA replication cell culture system. The most striking finding is that OSM exhibited synergistic inhibitory activity on interferon (IFN)-α even at a low concentration with weak anti-HCV activity, such as 25 pg/ml. OSM is a candidate anti-HCV reagent and may improve the current IFN therapy for patients with chronic hepatitis C.

1. Introduction

Currently the combination therapy of pegylated-interferon-α (PEG-IFN-α) with ribavirin (RBV) is available for patients with chronic hepatitis C (CH C). However, the sustained virological response (SVR) rate is still approximately 55% [1]. There is thus an urgent need for novel partners for IFN.

Oncostatin M (OSM) belongs to the interleukin (IL)-6 family, which also includes IL-6, IL-11, IL-27, ciliary neurotrophic factor, cardiotrophin-like cytokine, cardiotrophin-1, neuropoietin and leukemia-inhibitory factor (LIF) [2,3]. OSM was first reported as a cytokine produced from U-937 lymphoma cells, when it was found to inhibit the growth of melanoma cells [4]. The IL-6 family members share glycoprotein 130 (gp130) for signal transduction, and the OSM receptor consists of gp130 and its unique OSMR [5]. Recently it was reported that the IL-31 receptor also contains OSMR and forms a heterodimer with IL31RA [6]. OSMR and gp130 are highly expressed in liver, and OSM plays a significant role in the differentiation and regeneration of liver [7,8]. Therefore, OSM was used as a reagent for the differentiation of hepatocytes in vitro.

Here, we have found that OSM's anti-hepatitis C virus (HCV) activity is a new function of this cytokine. OSM synergistically inhibited HCV RNA replication in combination with IFN-α even at a low concentration with weak anti-HCV activity (20% inhibition). OSM may improve the current PEG-IFN-α and RBV therapy for patients with CH C and provide a clue toward understanding the diverse sensitivity to IFN therapy.

2. Materials and methods

2.1. Compounds and antibodies

IFN-α was purchased from Sigma (St. Louis, MO). OSM and IL-31 were purchased from R&D Systems (Minneapolis, MN). IL-6 was purchased from Acris Antibodies (Herford, Germany). LIF was purchased from Chemicon International (Temecula, CA). Anti-HCV core antibody (CP11) was purchased from the Institute of Immunology (Tokyo, Japan), and anti-HCV non-structural 5A (NS5A) antibody was the generous gift of Dr. A. Takamizawa (Research Foundation for Microbial Diseases, Osaka University). Anti-β-actin antibody was purchased from Sigma. Anti-signal transducer and activator of transcription (STAT) 1 and anti-STAT3 antibodies were purchased from BD Bioscience (San Jose, CA). Anti-phospho-STAT1 (Y701) and anti-phospho-STAT3 (Y705) were purchased from Cell Signaling Technology (Danvers, MA).

Abbreviations: SVR, sustained virological response; CH C, chronic hepatitis C; EC_{50}, 50% effective concentration; EMCV, encephalomyocarditis virus; gp130, glycoprotein 130; HCV, hepatitis C virus; PEG-IFN, pegylated-interferon; IL, interleukin; IRES, internal ribosomal entry site; LIF, leukemia-inhibitory factor; NS, non-structural; OSM, oncostatin M; RBV, ribavirin; RL, *Renilla* luciferase; RT-PCR, reverse transcription-polymerase chain reaction; STAT, signal transducer and activator of transcription

* Corresponding author. Fax: +81 86 235 7392.
E-mail address: maikeda@md.okayama-u.ac.jp (M. Ikeda).

0014-5793/$36.00
doi:10.1016/j.febslet.2009.03.054

2.2. Cell culture

The OR6 cell line is cloned from ORN/C-5B/KE (strain O of genotype 1b) RNA replicating HuH-7 cells, as described previously [9]. OR6c cells are cured OR6 cells from which HCV RNA was eliminated by IFN-α treatment, as previously described [10]. HCV-O/RLGE (strain O) is the authentic HCV RNA containing adaptive mutations of Q1112R, P1115L, E1202G, and K1609E in the NS3 region and replicates efficiently in OR6c cells [11]. Li23 and PH5CH cells were cultured as previously described [12].

2.3. OR6 reporter assay

For the *Renilla* luciferase (RL) assay, 1.5×10^4 OR6 cells were plated onto 24-well plates in triplicate and pre-cultured for 24 h. The cells were treated with OSM and/or IFN-α for 72 h. After the treatment, the cells were harvested with *Renilla* lysis reagent (Promega, Madison, WI) and subjected to RL assay according to the manufacturer's protocol.

2.4. Cell growth assay

To examine OSM's activity in OR6 cell growth, 6.0×10^4 OR6 cells were plated onto 6-well plates in triplicate and were pre-cultured for 24 h. The cells were treated with OSM for 72 h, and then the number of viable cells was counted after trypan blue dye treatment, as previously described [13].

2.5. Reverse transcription and polymerase chain reaction (RT-PCR)

RT-PCR for gp130, OSMR, LIFR, IL6R, IL31RA and glyceraldehyde-3-phosphate dehydrogenase was performed by a method described previously [14]. Briefly, using cellular total RNAs (2 μg), cDNA was synthesized using M-MLV reverse transcriptase with oligo dT primer. One-tenth of the synthesized cDNA was subjected to PCR with the specific primer pairs (Supplementary materials).

2.6. Western blot analysis

For Western blot analysis to detect the expression of core and NS5A, 4×10^4 OR6c cells harboring HCV-O/RLGE RNA were plated onto 6-well plates and cultured for 24 h, and then were treated with IFN-α and/or OSM for 72 h. To detect the STATs and phosphorylated STATs, 5×10^5 OR6 cells were plated onto 6-well plates and cultured for 24 h, and then were treated with IFN-α and/or OSM. Preparation of the cell lysates, sodium dodecyl sulfate–polyacrylamide gel electrophoresis and immunoblotting were then performed as previously described [15].

3. Results

3.1. OSM inhibited HCV RNA replication in hepatoma cell line

We have tried to develop differentiated hepatocytes from mesenchymal stem cells using OSM as the differentiation reagent to establish the cell culture system for HCV RNA replication. We tested the reagents needed for differentiation, including OSM, to rule out negative activity for HCV RNA replication. In the course of this procedure, we happened to find that OSM possessed marked anti-HCV activity by using our developed full-length HCV RNA replication reporter system (OR6 assay system) [9]. This system enabled the prompt and precise evaluation of HCV RNA replication levels (Fig. 1A). OSM exhibited marked anti-HCV activity at a low concentration (50% effective concentration (EC_{50}): 0.71 ng/ml) (Fig. 1B) without cytotoxicity (Fig. 1C). OSM's anti-HCV activity was maintained at least until 96 h after a single administration of the reagent (Fig. 1D). These results indicate that OSM possesses anti-HCV activity at a concentration that

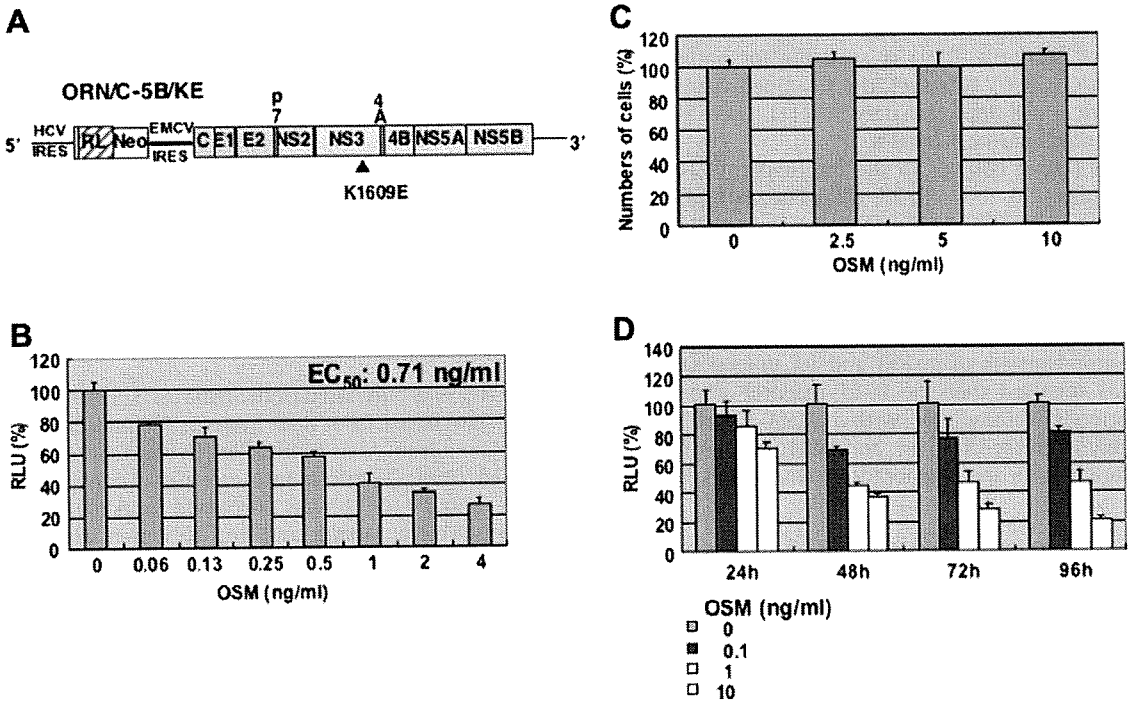

Fig. 1. Anti-HCV activity of OSM in HCV RNA replicating OR6 cells. (A) Schematic gene organization of the genome-length HCV RNA replicating in OR6 cells. The position of an adaptive mutation, K1609E, is indicated by a black triangle. (B) OR6 cells were treated with OSM for 72 h and subjected to RL assay. Relative luciferase unit (RLU) was calculated when the RL activity of the control was assigned as 100%. (C) OR6 cells were treated with OSM for 72 h and subjected to a cell viability assay with trypan blue staining. (D) OR6 cells were treated with OSM and harvested at 24, 48, 72, and 96 h and subjected to RL assay.

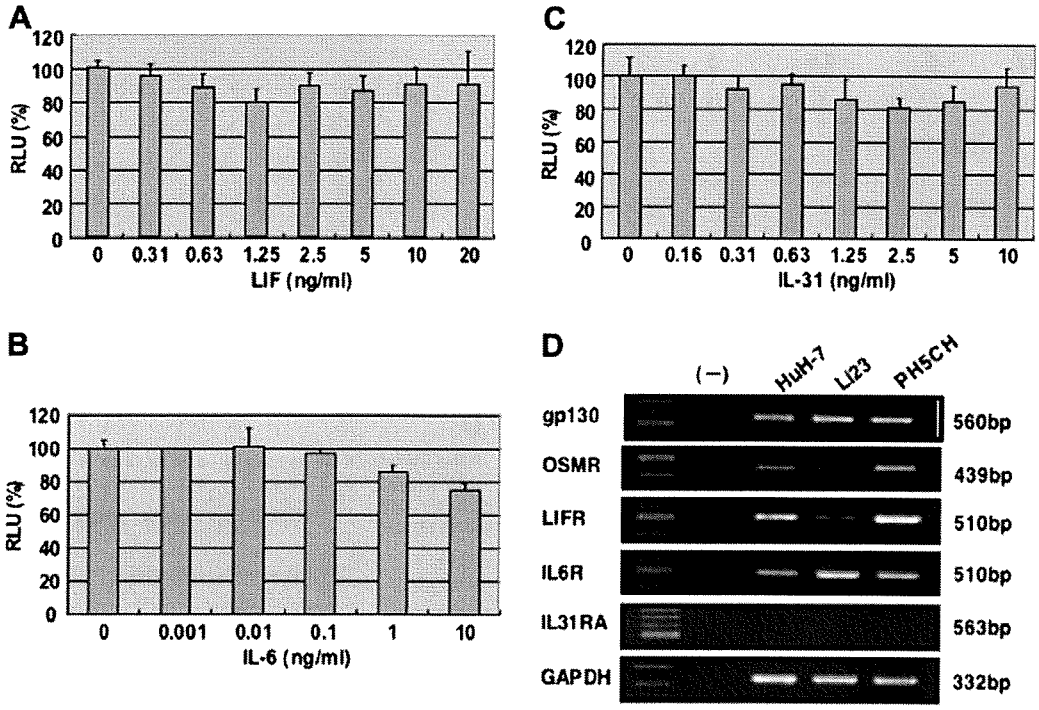

Fig. 2. The activities of LIF, IL-6 and IL-31 on HCV RNA replication. OR6 cells were treated with LIF (A), IL-6 (B) and IL-31 (C) for 72 h and subjected to RL assay. (D) RNAs from hepatocytes (HuH-7, Li23 and PH5CH) were subjected to RT-PCR with specific primer pairs to gp130, OSMR, LIFR, IL6R, IL31RA and GAPDH.

does not affect cell growth and is a new class of antiviral cytokine.

3.2. Anti-HCV activity of OSM is a unique feature in the IL-6 family

OSM belongs to the IL-6 family, whose members share the common gp130 molecule in each receptor [5]. Therefore, we next examined the activities of other representative IL-6 family members (LIF, IL-6) using the OR6 assay system. As shown in Fig. 2A, LIF had no effect on HCV RNA replication. IL-6 exhibited only a weak anti-HCV activity at the concentration of 10 ng/ml (approximately 20% inhibition) (Fig. 2B).

The OSM receptor consists of gp130 and OSMR [5]. IL31RA is another partner of OSMR and that the heterodimer of these molecules forms a receptor of IL-31 [6]. Therefore, we tried to determine whether or not IL-31 possesses anti-HCV activity in OR6 cells. The result revealed that IL-31 exhibited no anti-HCV activity. Next we examined the expression levels of the receptors in HuH-7, Li23 (a human hepatoma cell line) and PH5CH (an immortalized primary human hepatocyte line). All of these cell lines expressed gp130, OSMR, LIFR and IL6R but not IL31RA (Fig. 2D). The lack of 1L31RA expression resulted in IL-31 possessing no anti-HCV activity. These results suggest that OSM's anti-HCV activity seems to be a unique feature among IL-6 family members.

3.3. OSM synergistically enhanced anti-HCV activity of IFN-α

As HCV RNA contains three exogenous genes (RL, Neo and encephalomyocarditis virus (EMCV)-internal ribosomal entry site (IRES)) (Fig. 1A), we tried to determine whether OSM inhibits authentic HCV RNA replication in order to rule out the possibility that OSM's anti-HCV activity is not due to the inhibition of these exogenous genes. OSM inhibited core and NS5A expression in a dose-dependent manner (Fig. 3A, lanes 1–3). We next examined OSM's anti-HCV activity in combination with IFN-α using authentic HCV-O/RLGE RNA-replicating cells. OSM (1 and 10 ng/ml) drastically inhibited core and NS5A expression in combination with IFN-α (2.5, 5, and 10 IU/ml) (Fig. 3A, lanes 4–12).

OSM exhibited anti-HCV activity even at low concentrations, such as 62 pg/ml, and enhanced the anti-HCV activity of IFN-α (Fig. 3B). We also examined anti-HCV activity of CsA (0, 0.25, 0.5, and 1.0 μg/ml) alone or in combination with OSM (10 ng/ml) (Supplementary Fig. 1). OSM enhanced CsA's anti-HCV activity. Anti-HCV activity of OSM at 10 ng/ml was almost equal to that of CsA at 0.5 μg/ml. Then, we performed isobole plot analysis for EC_{50} of OSM and IFN-α. In Fig. 3C, dotted line means that the interaction of two reagents is evaluated as additive effect (or zero interaction). Points below this line correspond to synergistic interaction (or positive interaction) and points above this line indicate antagonism (or negative interaction) [16]. Therefore, isobole plot analysis of EC_{70} for OSM and IFN-α revealed that the combination of OSM and IFN-α exhibited striking synergistic inhibition of HCV RNA replication (Fig. 3C). Then we investigated whether or not OSM enhanced the IFN signaling pathway, since OSM activates STATs [17]. A kinetic study regarding the phosphorylation of STAT1 and STAT3 revealed that STAT1 (Y701) was markedly phosphorylated in the early phase within 60 min but that the phosphorylation level was reduced at 120 min (Fig. 3D). On the other hand, the phosphorylation of STAT1 by IFN-α remained consistent until 120 min after treatment (Fig. 3D). The phosphorylation kinetics of STAT3 (Y705) by OSM were consistent until 120 min (Fig. 3D). These results suggest that early-phase activation of STAT1 by OSM may trigger the synergistic activity in HCV RNA replication in combination with IFN-α.

3.4. OSM enhanced anti-HCV activity of IFN-α at even the low effective concentration by itself

As OSM exhibited marked synergistic anti-HCV activity with IFN-α, we tried to determine whether a low concentration of OSM could synergistically enhance the anti-HCV activity of IFN-

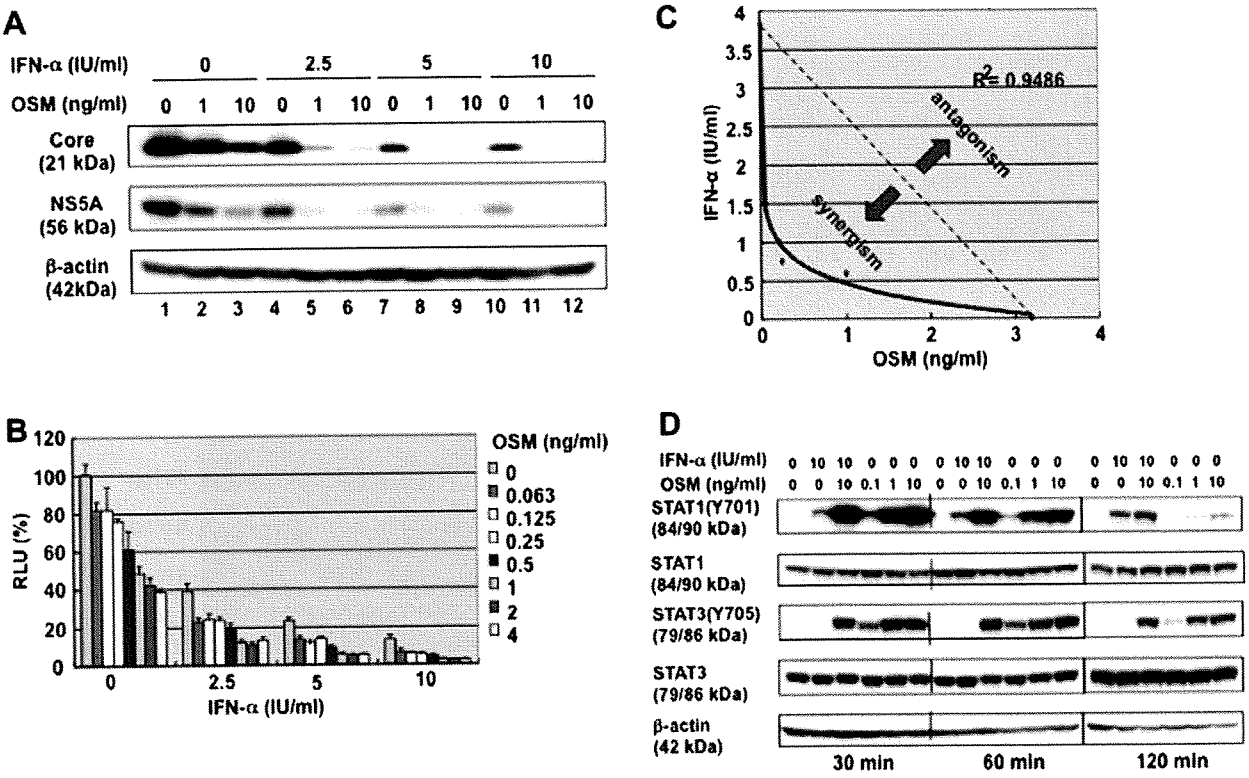

Fig. 3. Anti-HCV activity of OSM in combination with IFN-α. (A) HCV-O/RLGE-replicating OR6c cells were treated with OSM in combination with IFN-α for 96 h and subjected to Western blot analysis using anti-core, anti-NS5A and anti-β-actin antibodies. (B) OR6 cells were treated with OSM in combination with IFN-α for 72 h and subjected to RL assay. (C) Isobole plot analysis (EC_{70}) for OSM and IFN-α in OR6 cells after treatment for 72 h. (D) OR6 cells were treated with OSM and IFN-α for 30, 60 and 120 min and subjected to Western blot analysis using anti-STAT1, anti-phospho-STAT1 (Y701), anti-STAT3, anti-phospho-STAT3 (Y705) and anti-β-actin antibodies.

α. For this purpose, we treated OR6 cells with OSM at 25 pg/ml or 50 pg/ml in combination with IFN-α (0, 1, 2, 4, and 8 IU/ml). OSM alone at 25 pg/ml or 50 pg/ml exhibited only 20% inhibitory activity (Fig. 4A). However, OSM at these concentrations enhanced the anti-HCV activity of IFN-α up to 60% inhibition, when IFN-α at 8 IU/ml was treated with OSM at 25 pg/ml (Fig. 4B). These results

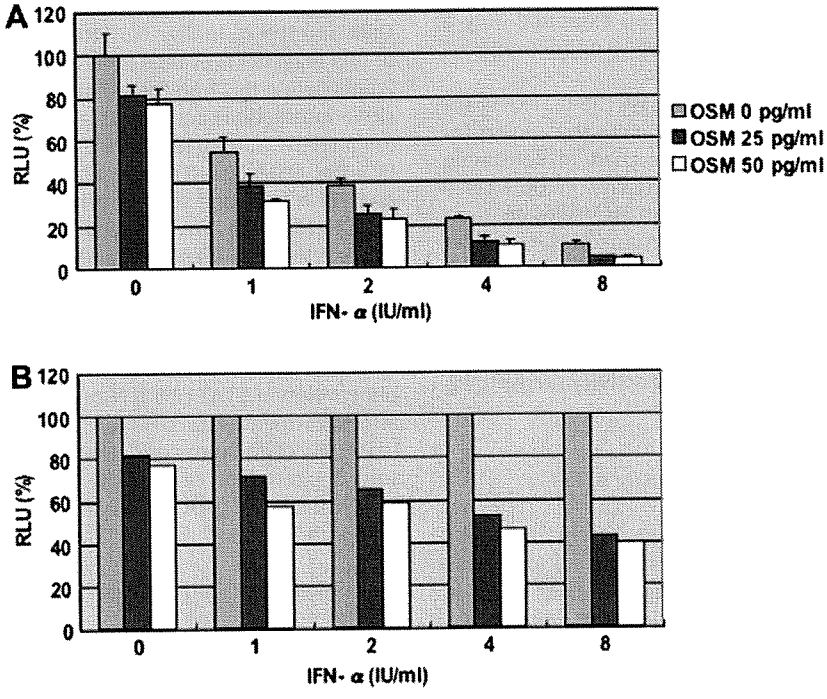

Fig. 4. OR6 cells were treated with OSM and IFN-α for 72 h and subjected to RL assay (A). Relative RL activity was adjusted when the RL activities of the cells treated with only IFN-α were assigned as 100% (B).

indicate that OSM is not only an anti-HCV reagent by itself but also a strong adjuvant for IFN-α's anti-HCV activity.

4. Discussion

In the present study, we found that OSM possesses anti-HCV activity, which constitutes a new function of this multi-functional cytokine. OSM is involved in liver regeneration and differentiation [7,8]. In the liver, OSM was produced by Kupffer cells [18], and the OSM signal was transmitted via its receptor, which consisted of gp130 and OMSR [5]. The IL-6 family members share gp130 in their receptors; it forms the heterodimer with a unique partner; for example IL6R in IL-6 and LIFR in LIF [2]. We tested the activity of LIF and IL-6 on HCV RNA replication. However, LIF did not exhibit anti-HCV activity, and IL-6 showed only weak anti-HCV activity compared to the OSM. These results suggest that OSM's anti-HCV activity is achieved via OSMR or the combination of gp130 and OSMR rather than via gp130. Recently, it was reported that IL31RA was another partner of OSMR in the IL-31 receptor [6]. If IL-31 could exhibit anti-HCV activity, OSMR seems to be significant in the signal transduction of anti-HCV activity. However, hepatocytes didn't seem to be a natural target of IL-31, because hepatocytes didn't express IL31RA. Further study is needed to clarify OSMR's role in anti-HCV activity.

Isobole plot analysis revealed that OSM exhibited a striking synergistic effect in the anti-HCV activity of IFN-α [19]. This synergistic activity of OSM may be caused by early strong activation of STAT1 by OSM. Furthermore, OSM enhanced the activity of 2′–5′ oligoadenylate synthetase promoter in combination with IFN-α (data not shown). These results suggest that STAT1 may be the key player in the synergy between OSM and IFN-α.

In this study, we found OSM's synergistic activity in the anti-HCV activity of IFN-α, when OSM was used at a low concentration (25 pg/ml) with only 20% inhibitory activity against HCV RNA replication. Surprisingly, OSM at 25 pg/ml enhanced the anti-HCV activity of IFN-α by up to 60%. RBV is the only adjuvant to the current PEG-IFN-α therapy for patients with CH C, and the combination therapy of PEG-IFN-α/RBV achieved only approximately 55% of the SVR rate. Therefore, OSM will become a strong partner to the current IFN therapy. As OSM strongly affected the anti-HCV activity of IFN-α, the serum concentration of OSM will affect the SVR in IFN therapy. The future study regarding the relationship between the serum concentration of OSM and SVR may provide a clue toward understanding the resistance to IFN therapy, and the development of OSM as a clinical reagent will serve as a breakthrough in therapy for patients with CH C.

In conclusion, we found OSM's anti-HCV activity a newly identified function of this multifunctional cytokine. The highlight of this study is that OSM exhibited a synergistic effect on the anti-HCV activity of IFN-α even at a low concentration with weak anti-HCV activity by itself.

Acknowledgments

The authors would like to thank Atsumi Morishita and Takashi Nakamura for their technical assistance. This work was supported by grants-in-aid for a third-term comprehensive 10-year strategy for cancer control and for research on hepatitis from the Ministry of Health, Labor and Welfare of Japan.

Appendix A. Supplementary material

Supplementary data associated with this article can be found, in the online version, at doi:10.1016/j.febslet.2009.03.054.

References

[1] Fried, M.W. et al. (2002) Peginterferon alfa-2a plus ribavirin for chronic hepatitis C virus infection. New Engl. J. Med. 347, 975–982.
[2] Heinrich, P.C., Behrmann, I., Haan, S., Hermanns, H.M., Muller-Newen, G. and Schaper, F. (2003) Principles of interleukin (IL)-6-type cytokine signalling and its regulation. Biochem. J. 374, 1–20.
[3] Rose, T.M. and Bruce, A.G. (1991) Oncostatin M is a member of a cytokine family that includes leukemia-inhibitory factor, granulocyte colony-stimulating factor, and interleukin 6. Proc. Natl. Acad. Sci. USA 88, 8641–8645.
[4] Zarling, J.M., Shoyab, M., Marquardt, H., Hanson, M.B., Lioubin, M.N. and Todaro, G.J. (1986) Oncostatin M: a growth regulator produced by differentiated histiocytic lymphoma cells. Proc. Natl. Acad. Sci. USA 83, 9739–9743.
[5] Mosley, B., De Imus, C., Friend, D., Boiani, N., Thoma, B., Park, L.S. and Cosman, D. (1996) Dual oncostatin M (OSM) receptors. Cloning and characterization of an alternative signaling subunit conferring OSM-specific receptor activation. J. Biol. Chem. 271, 32635–32643.
[6] Dillon, S.R. et al. (2004) Interleukin 31, a cytokine produced by activated T cells, induces dermatitis in mice. Nat. Immunol. 5, 752–760.
[7] Hamada, T. et al. (2007) Oncostatin M gene therapy attenuates liver damage induced by dimethylnitrosamine in rats. Am. J. Pathol. 171, 872–881.
[8] Kinoshita, T., Sekiguchi, T., Xu, M.J., Ito, Y., Kamiya, A., Tsuji, K., Nakahata, T. and Miyajima, A. (1999) Hepatic differentiation induced by oncostatin M attenuates fetal liver hematopoiesis. Proc. Natl. Acad. Sci. USA 96, 7265–7270.
[9] Ikeda, M., Abe, K., Dansako, H., Nakamura, T., Naka, K. and Kato, N. (2005) Efficient replication of a full-length hepatitis C virus genome, strain O, in cell culture, and development of a luciferase reporter system. Biochem. Biophys. Res. Commun. 329, 1350–1359.
[10] Ikeda, M., Abe, K., Yamada, M., Dansako, H., Naka, K. and Kato, N. (2006) Different anti-HCV profiles of statins and their potential for combination therapy with interferon. Hepatology 44, 117–125.
[11] Abe, K., Ikeda, M., Dansako, H., Naka, K. and Kato, N. (2007) Cell culture-adaptive NS3 mutations required for the robust replication of genome-length hepatitis C virus RNA. Virus Res. 125, 88–97.
[12] Kato, N., Ikeda, M., Mizutani, T., Sugiyama, K., Noguchi, M., Hirohashi, S. and Shimotohno, K. (1996) Replication of hepatitis C virus in cultured non-neoplastic human hepatocyte. Jpn. J. Cancer Res. 87, 787–792.
[13] Naka, K., Ikeda, M., Abe, K., Dansako, H. and Kato, N. (2005) Mizoribine inhibits hepatitis C virus RNA replication: effect of combination with interferon-alpha. Biochem. Biophys. Res. Commun. 330, 871–879.
[14] Dansako, H., Naganuma, A., Nakamura, T., Ikeda, F., Nozaki, A. and Kato, N. (2003) Differential activation of interferon-inducible genes by hepatitis C virus core protein mediated by the interferon stimulated response element. Virus Res. 97, 17–30.
[15] Kato, N. et al. (2003) Establishment of a hepatitis C virus subgenomic replicon derived from human hepatocytes infected in vitro. Biochem. Biophys. Res. Commun. 306, 756–766.
[16] Suhnel, J. (1990) Evaluation of synergism or antagonism for the combined action of antiviral agents. Antiviral Res. 13, 23–39.
[17] Mahboubi, K. and Pober, J.S. (2002) Activation of signal transducer and activator of transcription 1 (STAT1) is not sufficient for the induction of STAT1-dependent genes in endothelial cells. Comparison of interferon-gamma and oncostatin M. J. Biol. Chem. 277, 8012–8021.
[18] Znoyko, I., Sohara, N., Spicer, S.S., Trojanowska, M. and Reuben, A. (2005) Expression of oncostatin M and its receptors in normal and cirrhotic human liver. J. Hepatol. 43, 893–900.
[19] Yano, M., Ikeda, M., Abe, K., Dansako, H., Ohkoshi, S., Aoyagi, Y. and Kato, N. (2007) Comprehensive analysis of the effects of ordinary nutrients on hepatitis C virus RNA replication in cell culture. Antimicrob. Agents Chemother. 51, 2016–2027.

Oxidative Stress Induces Anti-Hepatitis C Virus Status via the Activation of Extracellular Signal-Regulated Kinase

Masahiko Yano,[1,3] Masanori Ikeda,[1] Ken-ichi Abe,[1] Yoshinari Kawai,[1,2] Misao Kuroki,[1] Kyoko Mori, [1] Hiromichi Dansako,[1] Yasuo Ariumi,[1] Shougo Ohkoshi,[3] Yutaka Aoyagi,[3] and Nobuyuki Kato[1]

Recently, we reported that β-carotene, vitamin D_2, and linoleic acid inhibited hepatitis C virus (HCV) RNA replication in hepatoma cells. Interestingly, in the course of the study, we found that the antioxidant vitamin E negated the anti-HCV activities of these nutrients. These results suggest that the oxidative stress caused by the three nutrients is involved in their anti-HCV activities. However, the molecular mechanism by which oxidative stress induces anti-HCV status remains unknown. Oxidative stress is also known to activate extracellular signal-regulated kinase (ERK). Therefore, we hypothesized that oxidative stress induces anti-HCV status via the mitogen activated protein kinase (MAPK)/ERK kinase (MEK)–ERK1/2 signaling pathway. In this study, we found that the MEK1/2-specific inhibitor U0126 abolished the anti-HCV activities of the three nutrients in a dose-dependent manner. Moreover, U0126 significantly attenuated the anti-HCV activities of polyunsaturated fatty acids, interferon-γ, and cyclosporine A, but not statins. We further demonstrated that, with the exception of the statins, all of these anti-HCV nutrients and reagents actually induced activation of the MEK–ERK1/2 signaling pathway, which was inhibited or reduced by treatment not only with U0126 but also with vitamin E. We also demonstrated that phosphorylation of ERK1/2 by cyclosporine A was attenuated with *N*-acetylcysteine treatment and led to the negation of inhibition of HCV RNA replication. We propose that a cellular process that follows ERK1/2 phosphorylation and is specific to oxidative stimulation might lead to down-regulation of HCV RNA replication. *Conclusion:* Our results demonstrate the involvement of the MEK–ERK1/2 signaling pathway in the anti-HCV status induced by oxidative stress in a broad range of anti-HCV reagents. This intracellular modulation is expected to be a therapeutic target for the suppression of HCV RNA replication. (HEPATOLOGY 2009;50: 678-688.)

Hepatitis C virus (HCV), which belongs to the family Flaviviridae, is a single-stranded positive-sense RNA virus of approximately 9.6 kb.[1,2] Persistent infection with HCV causes chronic hepatitis, which often leads to liver cirrhosis and hepatocellular carcinoma.[3] Therefore, HCV infection is a major health problem worldwide. Interferon (IFN)-based therapies, including the combination of pegylated IFN with ribavirin, are the current standard strategies for chronic hepatitis, but their sustained virological response rates are unsatisfactory.[4,5] There is thus an urgent need for novel partners with IFN or more effective reagents that may improve the sustained virological response rate.

Following the development in 1999 of a cell culture system to support efficient HCV RNA replication,[6] numerous studies have identified reagents that inhibit HCV RNA replication and enhance the effect of IFN treatment.[7-9] Some of these reagents are already available for clinical use. Previously, we also developed a genome-length HCV RNA (strain O of genotype 1b) replication system (OR6) with Renilla luciferase (RL) as a reporter in hepatoma cell lines.[10] Using this OR6 assay system, we found that mizoribine,[11] as an immunosuppressant, and

Abbreviations: AA, arachidonic acid; BC, β-carotene; CsA, cyclosporine A; CyPA, cyclophilin A; DHA, docosahexaenoic acid; DMSO, dimethyl sulfoxide; EGF, epidermal growth factor: EPA, eicosapentaenoic acid; ERK, extracellular signal-regulated kinase; FBS, fetal bovine serum; FLV, fluvastatin; HCV, hepatitis C virus; IFN, interferon; LA, linoleic acid: MAPK, mitogen-activated protein kinase; MEK, MAPK/ERK kinase; NS5A, nonstructural 5A; PTV, pitavastatin; PUFA, polyunsaturated fatty acid; RL, renilla luciferase; ROS, reactive oxygen species; VD2, vitamin D_2; VE, vitamin E.

From the Departments of [1]Tumor Virology and [2]Gastroenterology and Hepatology, Okayama University Graduate School of Medicine, Dentistry, and Pharmaceutical Sciences, Okayama, Japan; and the [3]Division of Gastroenterology and Hepatology, Graduate School of Medical and Dental Sciences, Niigata University, Niigata City, Japan.

Received August 5, 2008; accepted April 8, 2009.

Supported by grants-in-aid for a third-term comprehensive 10-year strategy for cancer control and for research on hepatitis from the Ministry of Health, Labor, and Welfare of Japan. K. A. was supported by a Research Fellowship from the Japan Society for the Promotion of Science for Young Scientists.

Address reprint requests to: Masanori Ikeda, Department of Tumor Virology, Okayama University Graduate School of Medicine, Dentistry, and Pharmaceutical Sciences, 2-5-1 Shikata-cho, Okayama 700-8558, Japan. E-mail: maikeda@md.okayama-u.ac.jp; fax: (81)-86-235-7392.

Published online in Wiley InterScience (www.interscience.wiley.com).

DOI 10.1002/hep.23026

Potential conflicts of interest: Nothing to report.

Additional Supporting Information may be found in the online version of this article.

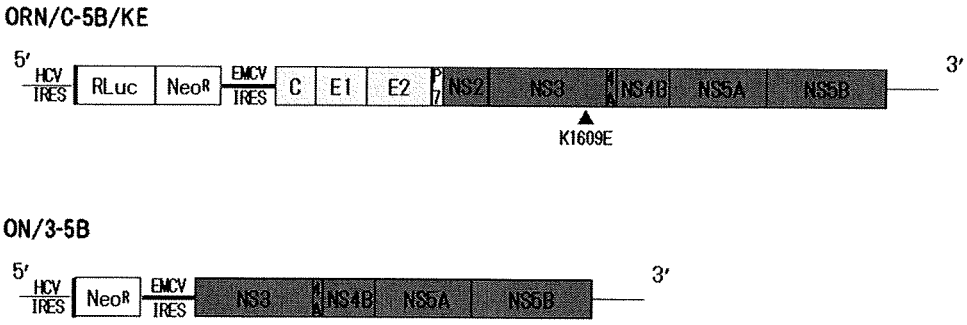

Fig. 1. Schematic gene organization of the genome-length and subgenomic HCV RNA used in this study. ORN/C-5B/KE encoding the RL gene was replicated in OR6 cells and ON/3-5B in sO cells. RL in OR6 cells was expressed as a fusion protein with neomycin phosphotransferase (Neo^R). The arrowhead indicates the position of K1609E, an adaptive mutation.

fluvastatin (FLV) and pitavastatin (PTV),[9,12] as the reagents for hypercholesterolemia, suppressed genome-length HCV RNA replication. Furthermore, in a recent study[13] in which we comprehensively analyzed the activities of ordinary nutrients on HCV RNA replication, three nutrients, β-carotene (BC), vitamin D_2 (VD2), and linoleic acid (LA), were found to suppress HCV RNA replication and enhance the antiviral activity of IFN-α or cyclosporine A (CsA) in an additive or a synergistic manner. Because the anti-HCV activities of these three nutrients, as well as CsA, were canceled by treatment with antioxidants such as vitamin E (VE) or selenium, we suggested that oxidative stress might be involved in the anti-HCV activities of these three nutrients and CsA. However, the detailed molecular mechanism via which the oxidative effects of these three nutrients and CsA suppress HCV RNA replication has not been explored.

The production of reactive oxygen species (ROS) plays a pivotal role in various cellular processes, including cell proliferation, differentiation, and apoptosis.[14] Whereas high-level production of ROS resulting from external stimuli is recognized as an important component of the pathogenesis of inflammatory and cancerous diseases, endogenously produced ROS at low concentrations are shown to function as signaling mediators of cellular responses.[15,16] Emerging evidence indicates that these ROS-triggered responses are mediated primarily via cellular signaling cascades, including a signaling pathway of extracellular signal-regulated kinase (ERK)1/2, namely p44/42 mitogen-activated protein kinase (MAPK), which belongs to the MAPK family.[17,18]

Several studies have revealed that certain viral proteins initiate activation of the MAPK/ERK kinase (MEK)–ERK1/2 signaling pathway, which may facilitate the viral replication and infectivity in the infected cells.[19,20] The HCV core protein[21] and the envelope protein[22] have also been reported to up-regulate this signaling pathway. However, another study reported that the HCV nonstructural 5A (NS5A) protein suppressed activating protein-1 activation by inhibiting the phosphorylation of ERK1/2 in replicon cells.[23] Moreover, recent studies using an inhibitor specific to the MEK–ERK1/2 signaling pathway reported that the direct anti-HCV activities of IFN-γ[24] and acetylsalicylic acid[25] are mediated in part through the induction of this cascade.

We demonstrate that the activation of MEK–ERK1/2 signaling plays a significant role in the anti-HCV activity caused by oxidative stress in a broad range of anti-HCV reagents.

Materials and Methods

Reagents and Antibodies. Dimethyl sulfoxide (DMSO), BC, VD2, VE, LA, arachidonic acid (AA), eicosapentaenoic acid (EPA), docosahexaenoic acid (DHA), and IFN-γ were purchased from Sigma Aldrich (St. Louis, MO), and CsA, FLV, U0126, PD98059, SB203580, and c-Jun N-terminal kinase inhibitor II were obtained from Calbiochem (San Diego, CA). Epidermal growth factor (EGF) was purchased from Toyobo (Osaka, Japan). PTV was purchased from Kowa Company, Ltd. (Tokyo, Japan). Anti-HCV core antibody (CP11) was purchased from the Institute of Immunology (Tokyo, Japan), and anti-HCV NS5A antibody was the generous gift of Dr. A. Takamizawa (Research Foundation for Microbial Diseases, Osaka University). Antibodies specific to ERK1/2 (p44/42 MAPK), MEK1/2, and phosphorylated (S217/221) MEK1/2 were purchased from Cell Signaling Technology (Beverly, MA), and anti-phosphorylated (T202/Y204) ERK1/2 antibody was obtained from BD Biosciences (San Jose, CA). Anti-β-actin antibody was purchased from Sigma Aldrich.

Cell Cultures. The cell lines OR6 and sO were cloned from ORN/C-5B/KE RNA and subgenomic replicon RNA (ON/3-5B)–replicating cells, respectively (Fig. 1). These cells were derived from the hepatoma cell line HuH-7, cultured in Dulbecco's modified Eagle's medium supplemented with 10% fetal bovine serum (FBS), peni-

cillin, streptomycin, and 300 μg/mL of G418 (Geneticin; Invitrogen, Carlsbad, CA), and passaged twice a week at a 5:1 split ratio. ORN/C-5B/KE and ON/3-5B were derived from HCV-O (strain O of genotype 1b).[10]

OR6 Reporter Assay. For the RL assay, 1.0-1.5 × 10^4 OR6 cells were plated onto 24-well plates in triplicate and precultured for 24 hours. The cells were pretreated with DMSO or a specific inhibitor for 1 hour and then were treated with each anti-HCV nutrient or compound in either the absence (DMSO) or presence of a specific inhibitor for 72 hours. After the treatment, the cells were harvested with Renilla lysis reagent (Promega, Madison, WI) and subjected to RL assay according to the manufacturer's protocol.

Western Blot Analysis. For analysis of the effect of a specific inhibitor on the anti-HCV activity, 6.0-6.5 × 10^4 OR6 cells were plated onto 6-well plates and precultured for 24 hours. The pretreatment with DMSO or a specific inhibitor for 1 hour and subsequent treatment for 72 hours was performed in the same manner as for the OR6 reporter assay. For analysis of the activities of each anti-HCV nutrient or reagent on the MEK–ERK1/2 signaling pathway, 1.0 × 10^5 OR6 or sO cells were plated onto 6-well plates and precultured in 10% FBS-containing medium for 24 hours. After the preculture, the culture medium was changed to FBS-free medium and the cells were cultured for 48 hours prior to treatment with each nutrient or reagent. When the effect of a specific inhibitor or VE on ERK1/2 phosphorylation was analyzed, the cells were pretreated with the specific inhibitor or VE for 1 hour prior to each treatment. Preparation of the cell lysates, sodium dodecyl sulfate–polyacrylamide gel electrophoresis, and immunoblotting were then performed as described.[26]

Measurement of ROS. OR6 cells in 24-well plates were left untreated or were treated with hydrogen peroxide (1 mM), LA (200 μM), and CsA (15 μg/mL) for 30 minutes and then incubated with dihydrodichlorocarboxyfluorescein diacetate (Invitrogen) (5 μM) for 15 minutes. Fluorescence was measured with a FLUOROSKAN ASCENT fluorescence plate reader (Thermo Fisher Scientific, Waltham, MA) at an excitation wavelength of 485 nm and emission wavelength of 535 nm.

Cell Growth Assay. To examine the activity of EGF on OR6 cell growth, 6.0-6.5 × 10^4 OR6 cells were plated onto 6-well plates in triplicate and were pre-cultured for 24 hours. The cells were treated with or without EGF for 72 hours, and the number of viable cells was counted after trypan blue dye treatment as described.[11]

Statistical Analysis. Statistical comparison of the luciferase activities between the various treatment groups was performed using the Student *t* test. *P* values of less than 0.05 were considered statistically significant.

Results

Effects of MEK1/2-Specific Inhibitors on the Anti-HCV Activities of BC, VD2, and LA in OR6 Cells. Our recent study suggested the involvement of oxidative stress in the suppressive mechanism of three anti-HCV nutrients: BC, VD2, and LA.[13] Because there have been reports of negative regulation of HCV RNA replication via the MEK–ERK1/2 signaling pathway,[24,25] which is one of the oxidative stress-induced cellular signaling pathways, we hypothesized that the suppression of HCV RNA replication by these three nutrients might be mediated via this cascade (Supporting Fig. 1). To test this hypothesis, we first used an OR6 assay system to examine the effects of U0126 and PD98059, inhibitors specific to MEK1/2, on the three anti-HCV nutrients at 60% inhibitory concentration. As shown in Fig. 2A, treatment with either 5 μM of U0126 or 10 μM of PD98059 slightly enhanced HCV RNA replication in comparison with the control. However, U0126 attenuated the anti-HCV activities of the three nutrients more clearly than PD98059 (Fig. 2A,B). U0126 prevented the anti-HCV activities of the three nutrients in a significant and dose-dependent manner and exerted complete inhibition against the anti-HCV activities of BC and LA (Fig. 2C,D), while the inhibitory effect of PD98059 was more mild (Fig. 2E,F). As shown in Fig. 2G, we also found that U0126 treatment restored the expressions of HCV proteins, core, and NS5A in a dose-dependent manner. We further demonstrated that knockdown of MEK1 or MEK2 by small interfering RNA negated the anti-HCV activity of LA (Supporting Fig. 2A-C). These inhibitions by U0126 against the anti-HCV activities of the three nutrients were not due to the enhancement of encephalomyocarditis virus/internal ribosomal entry site–driven RL activity, because this activity was not increased by U0126 (data not shown). Moreover, treatment with neither SB203580 (an inhibitor specific to p38 MAPK) nor c-Jun N-terminal kinase inhibitor, both of which belong to the same cascade family as MEK–ERK1/2, significantly affected the anti-HCV activities of the three nutrients (data not shown). These results imply that the activation of the MEK–ERK1/2 signaling pathway might be required for the suppression of genome-length HCV RNA replication by the three nutrients in cell culture.

Effect of U0126 on the Suppressive Effects of Polyunsaturated Fatty Acids and Anti-HCV Reagents in OR6 Cells. Previous studies using a cell culture system have shown that polyunsaturated fatty acids (PUFAs), including LA, act as anti-HCV nutrients.[27,28] A recent study reported that lipid peroxidation of PUFAs was correlated with their anti-HCV activities, which were pre-

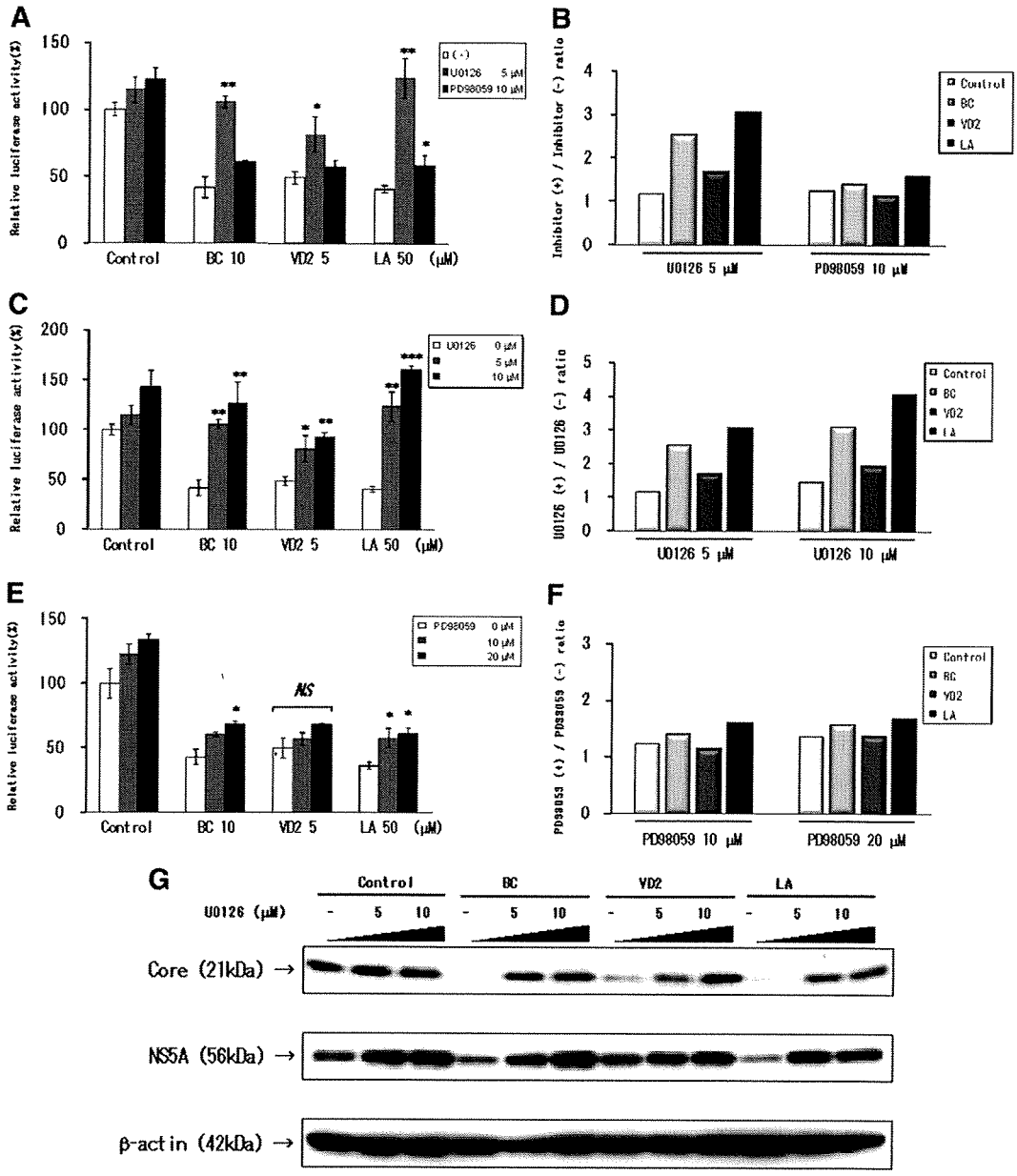

Fig. 2. U0126 strongly inhibited the anti-HCV activities of the anti-HCV nutrients BC, VD2, and LA in OR6 cells. (A,B) Effects of MEK-specific inhibitors on the three nutrients at the 60% inhibitory concentration. OR6 cells were pretreated with DMSO, 5 μM U0126, or 10 μM PD98059 for 1 hour. The cells were then treated with control medium, 10 μM BC, 5 μM VD2, or 50 μM LA in either the absence (DMSO) or presence of each specific inhibitor for 72 hours. After treatment, RL assay was performed as described in Materials and Methods. Shown here is the relative luciferase activity (%) calculated when the RL activity of the control was assigned as 100%. Data are expressed as the mean $\pm$ standard deviation of triplicate samples from at least three independent experiments. Asterisks indicate significant difference from treatment with DMSO ($*P < 0.05$; $*P < 0.01$) (A). The ratio of the RL activity in the presence of the MEK-specific inhibitor to the RL activity in the absence of the inhibitor was then calculated (B). (C-F) OR6 reporter assays of the dose effects of MEK1/2-specific inhibitors on the three nutrients. OR6 cells were pretreated with DMSO, U0126 (C), or PD98059 (E) at the indicated concentrations for 1 hour. Treatment of the cells with control medium or each of the three nutrients in either the absence (DMSO) or presence of each specific inhibitor and the RL assay of harvested OR6 cell samples were performed as described in panels A and B. Asterisks indicate significant difference from treatment with DMSO ($*P < 0.05$; $**P < 0.01$; $***P < 0.001$; NS, not significant). Next, we calculated the ratio of RL activity in the presence of the MEK-specific inhibitor, U0126 (D), or PD98059 (F), to the RL activity in the absence of the inhibitor. (G) Western blot analysis of the dose effects of U0126 on three nutrients. OR6 cells were pretreated and then treated as in panel C. The production of HCV core and NS5A in the cells was analyzed by way of immunoblotting using antibodies specific to HCV core (top row) and NS5A (middle row). β-actin was used as a control for the amount of protein loaded per lane (bottom row).

vented by treatment with VE.[29] This result coincides with our previous observations on the effects of LA.[13] We proposed that the MEK–ERK1/2 signaling pathway might be involved in the anti-HCV activity of PUFAs, including LA, because lipid peroxidation is known to be a ROS-triggered cellular modification.[16] As expected, treatment with U0126 attenuated the anti-HCV activities of four representative PUFAs in a significant and dose-dependent manner (Fig. 3A,B).

Moreover, because the anti-HCV activities of BC, VD2, LA, and CsA, but not FLV, were found to be negated by VE,[13] we were also interested in the potent role of the MEK–ERK1/2 signaling pathway in the anti-HCV mechanism of CsA. Furthermore, the previous study using a subgenomic replicon system had already shown the partial involvement of this cascade in the antiviral activity of IFN-γ.[24] Therefore, we examined the effects of U0126 on various anti-HCV reagents: IFN-γ, CsA, and statins (FLV and PTV). We confirmed that also in genome-length HCV RNA replication cells, U0126 significantly inhibited the anti-HCV activity of IFN-γ (Fig. 3C,D). Interestingly, consistent with the effects of treatment with VE,[13] the anti-HCV activity of CsA was completely abrogated by U0126 in a significant and dose-dependent manner, whereas statins were unaffected (Fig. 3C,D).

U0126 restored the reduced expression of HCV proteins by PUFAs, IFN-γ, and CsA in a dose-dependent manner, whereas statins were unaffected (Fig. 3E,F). These results were supported by additional real-time reverse-transcription polymerase chain reaction and immunofluorescence analyses (Supporting Fig. 3A-C). We also observed that knockdown of MEK1 or MEK2 by small interfering RNA did not affect the anti-HCV activity of PTV (Supporting Fig. 2A-C). Collectively, these findings suggest that the MEK–ERK1/2 signaling pathway may play a critical role in the negative regulation of HCV RNA replication by the anti-HCV nutrients BC and VD2, PUFAs, and the anti-HCV reagents IFN-γ and CsA, but not statins.

Activation of the MEK–ERK1/2 Signaling Pathway by Anti-HCV Nutrients and Reagents. To further ensure the involvement of the MEK–ERK1/2 signaling pathway in the suppressive mechanisms of anti-HCV nutrients and reagents, we next examined whether these nutrients and reagents could actually initiate the activation of this signaling pathway. After treating the HCV RNA replicating cells with each of the nutrients and reagents, we performed immunoblotting specific to the phosphorylation of ERK1/2 and MEK1/2. In the same way as EGF, a potent activator of these kinases, the three anti-HCV nutrients (BC, VD2, and LA) enhanced the phosphorylation of ERK1/2 and MEK1/2 in both genome-length and subgenomic HCV RNA replication cells (Fig. 4A,B). IFN-γ, CsA, and all of the PUFAs also up-regulated this cascade in OR6 cells (Fig. 4C,D). The increase in phosphorylation of ERK1/2 was not observed after either statin treatment (Fig. 4D). The activation of MEK–ERK1/2 by the three anti-HCV nutrients was apparent until 1 hour after their application and subsequently attenuated, although EGF exhibited persistent enhancement of MEK–ERK1/2 phosphorylation (Fig. 4E). Because the experiments regarding ERK1/2 phosphorylation were performed in FBS-free conditions, we checked the anti-HCV activity of PTV, CsA, and LA in FBS-free medium. The results revealed that these anti-HCV reagents and nutrients also inhibited HCV RNA replication in FBS-free conditions (Supporting Fig. 4). Taken together, these findings indicate that the anti-HCV nutrients and reagents activated the MEK–ERK1/2 signaling pathway in HCV RNA replicating cells, providing further confirmation that this signaling cascade might be involved in their anti-HCV activities.

MEK1/2-Specific Inhibitors Attenuated the Increased Phosphorylation of ERK1/2 by Anti-HCV Nutrients/Reagents and EGF. We next tested whether MEK1/2-specific inhibitors could prevent not only the suppression of HCV RNA replication but also the activation of ERK1/2 by the anti-HCV nutrients BC, VD2, and PUFAs and the anti-HCV reagents IFN-γ and CsA. Consistent with the inhibitory effects on their anti-HCV activities, U0126 more markedly abrogated the increase in ERK1/2 phosphorylation by anti-HCV nutrients, reagents, and EGF than did PD98059 (Fig. 5A,B). As shown in Fig. 5C, the enhanced ERK1/2 phosphorylation by the three nutrients and EGF was reduced by U0126 in a dose-dependent manner.

VE Attenuated the Increased Phosphorylation of ERK1/2 by Anti-HCV Nutrients/Reagents and EGF. Because the suppression of HCV RNA replication by BC, VD2, LA, and CsA were completely negated by the treatment with VE in our recent study,[13] we investigated whether VE could also inhibit ERK1/2 activation by anti-HCV nutrients and reagents. As expected, VE also attenuated the enhanced phosphorylation of ERK1/2 by not only anti-HCV nutrients and CsA but also IFN-γ and EGF (Fig. 6A,B). We also demonstrated that phosphorylation of ERK1/2 by CsA was attenuated with *N*-acetylcysteine treatment and led to the negation of inhibition of HCV RNA replication (Supporting Fig. 5A-C). The anti-HCV nutrients and reagents, whose activities were negated by U0126, were also inhibited by VE. In contrast, the anti-HCV activities of statins were not negated by U0126 or VE. We also demonstrated that LA and CsA induce ROS (Fig.

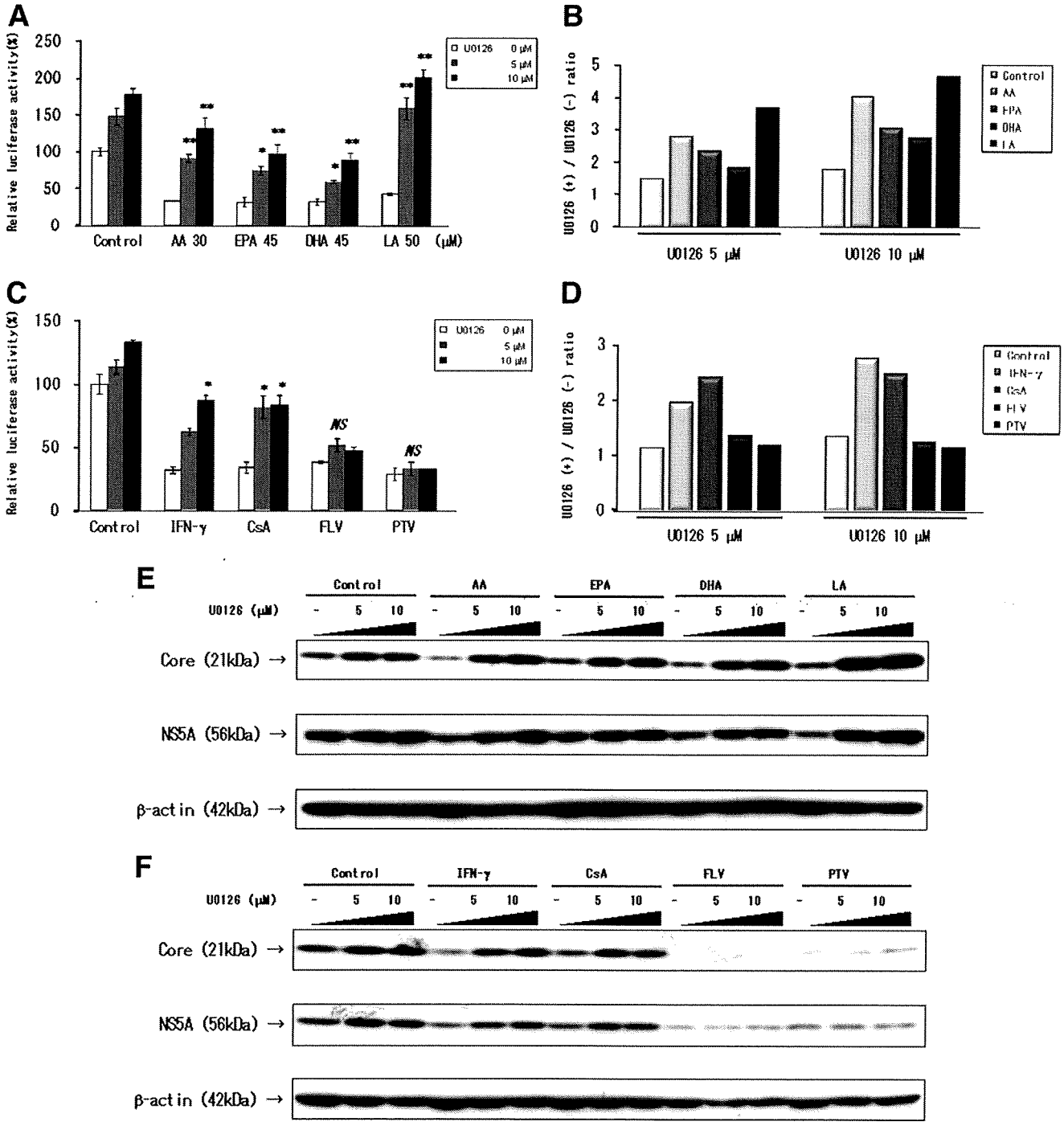

Fig. 3. U0126 dose-dependently attenuated the anti-HCV activities of PUFAs, IFN-γ, and CsA, but not the statins. (A-D) OR6 reporter assays of the dose effects of U0126 on the PUFAs and anti-HCV reagents at the 60% inhibitory concentration. OR6 cells were pretreated with DMSO or U0126 as in Fig. 2C and then treated with control medium, 30 μM AA, 45 μM EPA, 45 μM DHA, or 50 μM LA (A) and control medium, 0.4 IU/mL IFN-γ, 0.2 μg/mL CsA, 3 μM FLV, or 1 μM PTV (C), respectively, in either the absence (DMSO) or presence of U0126 for 72 hours. After the treatment, the RL assay of harvested OR6 cell samples was performed as described in Fig. 2A and 2B. Asterisks indicate significant difference from treatment with DMSO ($*P < 0.05$; $**P < 0.01$; NS, not significant). The ratio of the RL activity in the presence of U0126 to the RL activity in the absence of U0126 was then calculated (B, D). (E, F) Western blot analysis of the dose effects of U0126 on the PUFAs and anti-HCV reagents. The production of HCV core (top row) and NS5A (middle row) in the cells treated as in panel A (E) and panel C (F) was analyzed as described in Fig. 2G. β-actin was used as a control for the amount of protein loaded per lane (bottom row).

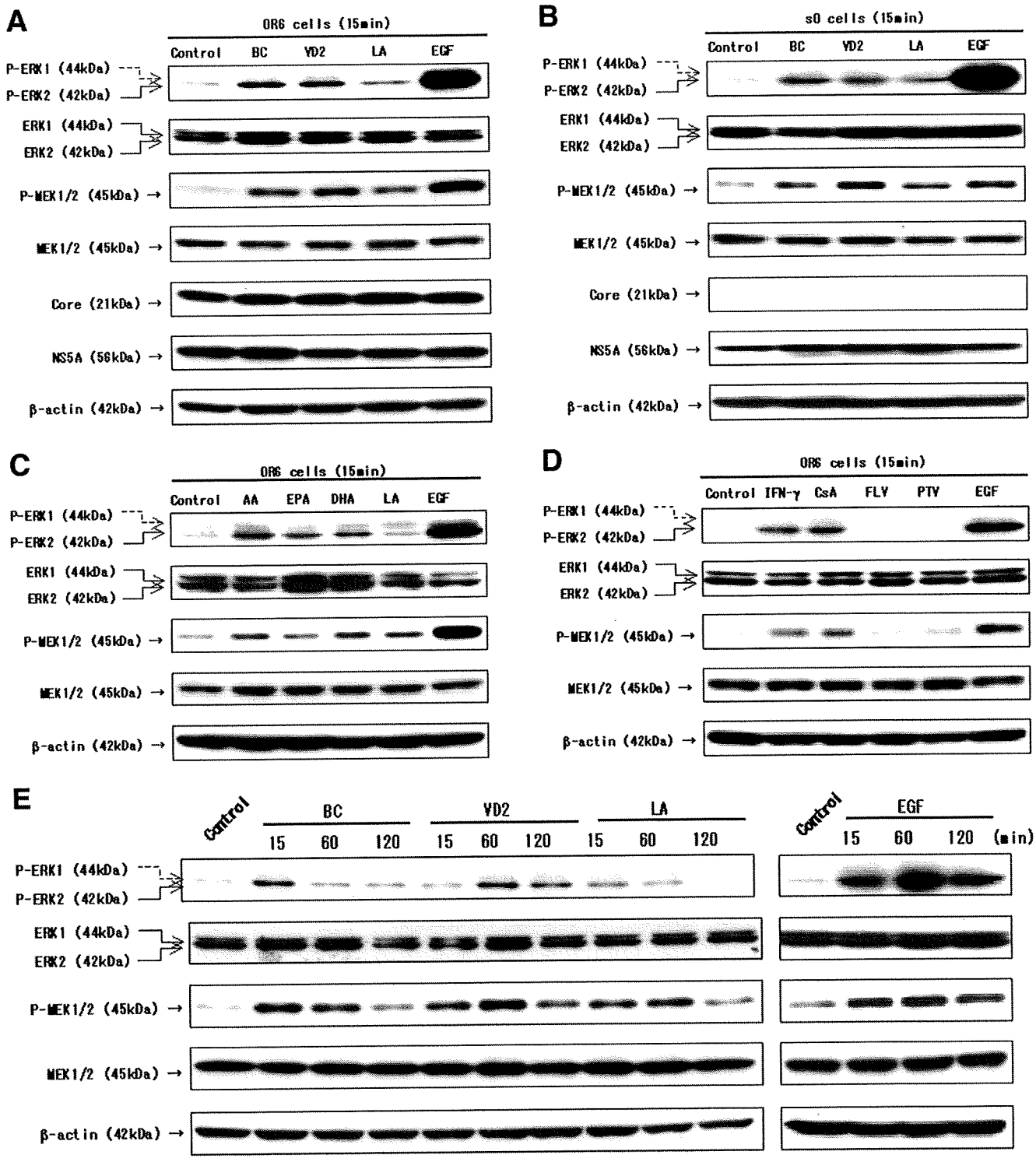

Fig. 4. U0126 attenuated the MEK-ERK1/2 signaling pathway activated by anti-HCV nutrients and reagents. (A, B) Three anti-HCV nutrients—BC, VD2, and LA—increased the phosphorylation of MEK-ERK1/2 in both full-length and subgenomic HCV RNA replication cells. OR6 cells (A) or sO cells (B) were maintained in FBS-free medium for 48 hours and then treated with control medium, 20 μM BC, 10 μM VD2, 100 μM LA, or 50 ng/mL EGF for 15 minutes. After treatment, cell lysates underwent western blot analysis using antibodies specific to phosphorylated ERK1/2, ERK1/2, phosphorylated MEK1/2, and MEK1/2. The appropriate expression of HCV core and NS5A was determined by way of immunoblotting with their respective antibodies. (C, D) IFN-γ, CsA, and the PUFAs, but not the statins, increased the phosphorylation of MEK-ERK1/2 in OR6 cells. OR6 cells were precultured as described in panels A and B, then treated with control medium, 100 μM AA, EPA, DHA, or LA, or 50 ng/mL EGF (C) and control medium, 2 IU/mL IFN-γ, 2 μg/mL CsA, 5 μM of FLV or PTV, or 50 ng/mL EGF (D), respectively, for 15 minutes. (E) Time-course western blot analysis of the increase of MEK-ERK1/2 phosphorylation by the three anti-HCV nutrients and EGF. Samples for analysis were harvested prior to treatment with the control medium, 20 μM BC, 10 μM VD2, 100 μM LA, or 50 ng/mL EGF (0 time point) and at 15, 60, and 120 minutes posttreatment. After all of the treatments (C-E), cell lysates were subjected to western blot analysis of the activation of the MEK-ERK1/2 signaling pathway as described in panels A and B. β-actin was used as a control for the amount of protein loaded per lane in all analyses.

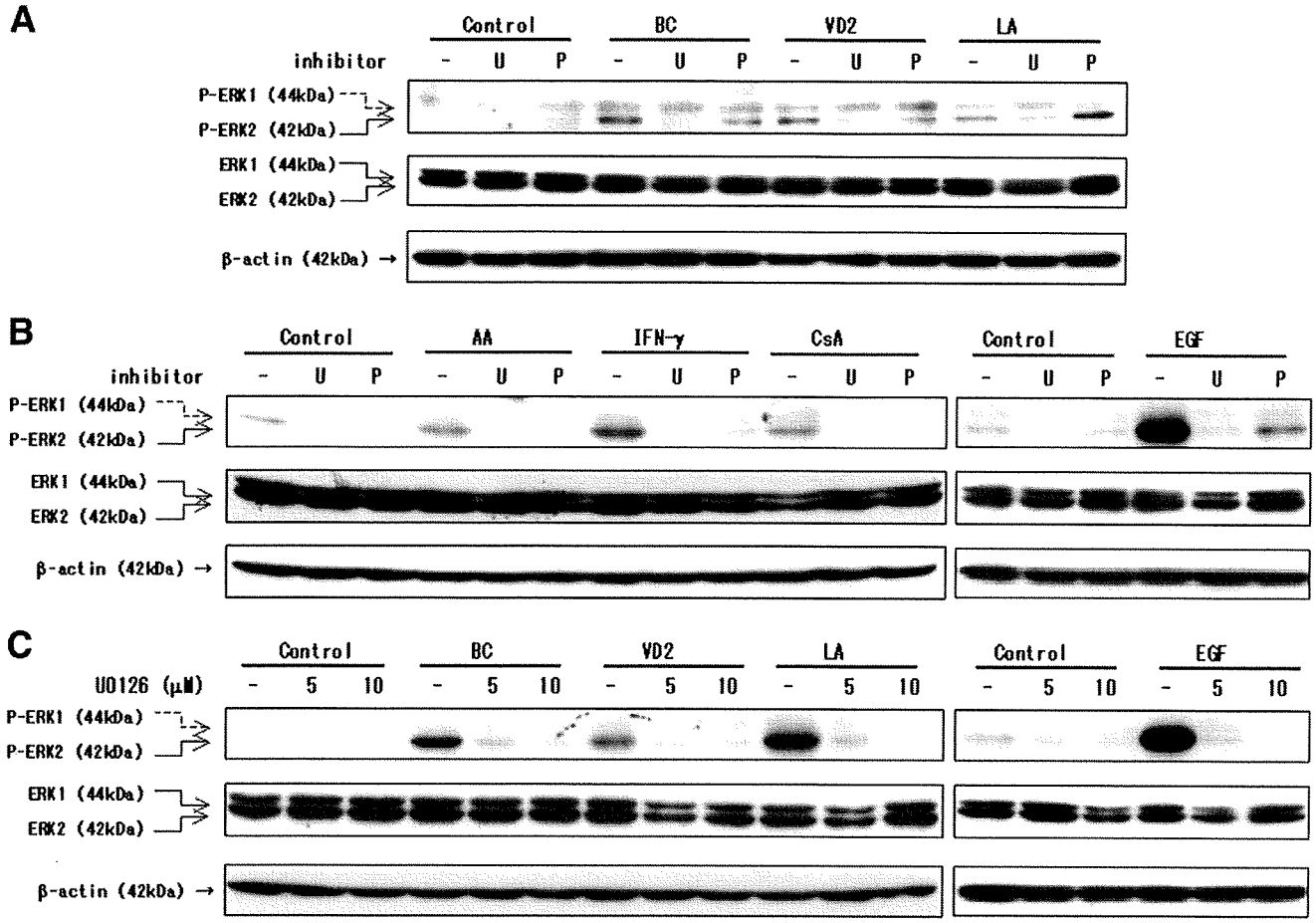

Fig. 5. U0126 strongly abolished ERK1/2 phosphorylation by the anti-HCV nutrients, anti-HCV reagents, and EGF. (A,B) Effects of the MEK1/2-specific inhibitors on ERK1/2 phosphorylation by anti-HCV nutrients and reagents. OR6 cells were precultured as described in Figs. 4A and B, and then pretreated with DMSO (−), 10 μM U0126: (U), or 20 μ M PD98059: (P) for 1 hour. Subsequently, the cells were treated with control medium, 20 μM BC, 10 μM VD2, or 100 μM LA (A) and control medium, 100 μM AA, 2 IU/mL IFN-γ, 2 μg/mL CsA, or 50 ng/mL EGF (B), respectively, in either the absence (DMSO) (−) or presence of U0126 (U) or PD98059 (P) for 15 minutes. (C) Dose effects of U0126 on ERK1/2 phosphorylation by the three anti-HCV nutrients and EGF. OR6 cells were precultured as described in Figs. 4A and 4B, then pretreated with DMSO (−) or 5 or 10 μM U0126 for 1 hour. The cells were then treated with control medium, 20 μM BC, 10 μM VD2, 100 μM LA, or 50 ng/mL EGF in either the absence (−) or presence of U0126 for 15 minutes. After all treatments (A-C), cell lysates were subjected to western blot analysis using antibodies specific to phosphorylated ERK1/2 (top row) and ERK1/2 (middle row). β-actin was used as a control for the amount of protein loaded per lane (bottom row).

7). Collectively, these results suggest that these nutrients and reagents induce ROS as an oxidant in HCV RNA replicating cells, leading to activation of the MEK–ERK1/2 signaling pathway and suppression of HCV RNA replication.

The Effects of EGF on HCV RNA Replication were Different than Those of the Anti-HCV Nutrients/Reagents. Because the study by Huang et al.[24] showed that EGF time-dependently suppressed the expressions of HCV nonstructural proteins in subgenomic replicon-harboring cells, we wondered whether EGF could suppress genome-length HCV RNA replication. EGF inhibited HCV RNA replication by approximately 25% at a concentration of 100 ng/mL. This anti-HCV activity was weaker than that of the anti-HCV nutrients and reagents tested in this study. However, as shown in the cell growth assay, EGF promoted OR6 cell proliferation in a dose-dependent manner (Supporting Fig. 6). These cell growth effects of EGF may have caused us to underestimate the actual anti-HCV activity of EGF. The other reagents and nutrients did not affect cell proliferation compared with EGF (Supporting Fig. 7).

Discussion

The previous studies using the MEK1/2-specific inhibitor and subgenomic replicon system showed that induction of the MEK–ERK1/2 signaling pathway might be required for the suppression of HCV RNA replication by some reagents.[24,25] In agreement with the study by Huang